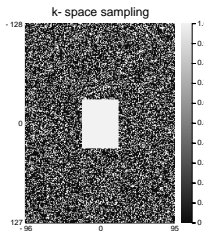


Jeffrey A. Fessler

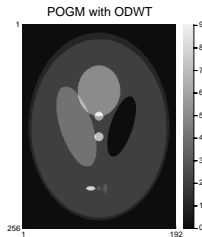
EECS Dept., BME Dept., Dept. of Radiology
University of Michigan



<http://web.eecs.umich.edu/~fessler>

SIAM Imaging Science 2020 Tutorial

2020-07-14



[1] <http://doi.org/10.1109/JPROC.2019.2936204>

Sai Ravishankar, Jong Chul Ye, J A Fessler. Image reconstruction: from sparsity to data-adaptive methods and machine learning. Proc. IEEE, 108(1):86-109, Jan. 2020.

[2] <http://doi.org/10.1109/MSP.2019.2943645>

J A Fessler. Optimization methods for MR image reconstruction.
IEEE Sig. Proc. Mag., 37(1):33-40, Jan. 2020.

[3] <http://arxiv.org/abs/1907.11818>

Il Yong Chun, Zhengyu Huang, Hongki Lim, J A Fessler. Momentum-Net: Fast and convergent iterative neural network for inverse problems. 2019.

Slides:

<https://web.eecs.umich.edu/~fessler/papers/files/talk/20/siam.pdf>

Introduction

Brief review of classic methods (> 10 years old)

Sparsity regularizers: Basic

Sparsity regularizers: Advanced

Adaptive regularizers

Denoising-based “regularization”

Deep-learning approaches for image reconstruction

Looking forward

Bibliography

Introduction

History

Scope

Code: Julia and Jupyter

Measurement model

Brief review of classic methods (> 10 years old)

Sparsity regularizers: Basic

Sparsity regularizers: Advanced

Adaptive regularizers

Denoising-based “regularization”

Deep-learning approaches for image reconstruction

Looking forward

Bibliography

- ▶ Goal of accelerating MRI scans has a long history
 - gradient waveforms: echo-planar imaging [4], echo-volumar imaging [5], spiral imaging [6, 7], ...
 - partial Fourier [8, 9, 10]
 - parallel imaging [11, 12, 13]
sensitivity encoded imaging, initially with regular under-sampling [14, 15, 16],
soon after with irregular / non-Cartesian sampling [17, 18]
 - Data-driven choice of phase encodes: Yue Cao & David Levin, 1993 [19]
recent work optimizes sampling patterns: [20, 21, 22, 23, 24, 25, 26, 27, 28]
- ▶ Recent history (since 2006) driven by compressed sensing
 - Conf. papers 2004-2006 [29, 30, 31, 32]
 - Journal papers in 2007 [33, 34, 35, 36]
 - Review papers (!) in 2008 [37] [38]
 - FDA approval for CS in MRI 10 years later [39, 40, 41, 42] "HyperSense" "Compressed SENSE"

Every great idea has its precursors: Y. Bresler's group was solving $\min_x \|x\|_0$ s.t. $\|\mathbf{A}x - \mathbf{b}\| \leq \varepsilon$ in 1998 [43]

- ▶ static vs dynamic imaging
- ▶ single-coil vs multiple-coil data (parallel MRI)
- ▶ “SENSE” methods model coil sensitivities in the image domain
- ▶ “GRAPPA” methods model the effect of coil sensitivity in k-space
- ▶ “calibrationless” methods that use low-rank properties [45, 46, 47]
- ▶ clinical anatomical imaging vs quantitative [48, 49, 50, 51]
- ▶ smooth vs non-smooth cost functions

- ▶ Jupyter notebooks with code in the language [Julia \[52\]](#) illustrate many of the methods shown in this tutorial
- ▶ Notebooks use the Michigan Image Reconstruction Toolbox in Julia (MIRT.jl)
<http://github.com/JeffFessler/MIRT.jl>
- ▶ For demo notebooks, see: <https://github.com/JeffFessler/mirt-demo>
- ▶ Installation-less test drives using <https://mybinder.org/>
- ▶ Matlab version of MIRT: <http://web.eecs.umich.edu/~fessler/code/index.html>

Why Julia?

- adopts best ideas of Matlab and Python (among others),
- interactive yet built on a compiler (solves “2 language problem”), ...
- open source, ...
- package manager facilitates exact reproducible research.
- My Julia tutorial: <https://www.ima.umn.edu/2019-2020/SW10.14-18.19/28302>

From <http://github.com/JeffFessler/MIRT.jl>

Examples

You can test drive some jupyter notebooks in your browser without installing any local software by using the free service at <https://mybinder.org/>

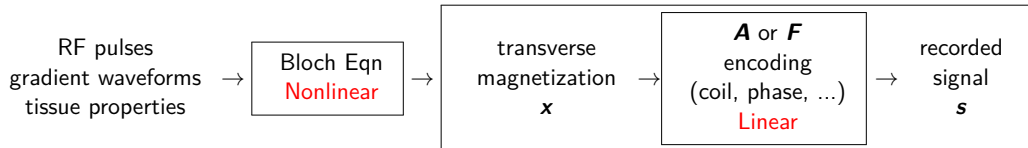
- Introduction: [!\[\]\(750841ae7100dc832cb0a4b3af4492f3_img.jpg\) launch binder](#)
- MRI compressed sensing demo: [!\[\]\(78e449f8a1164b81ecbd00cd97498e27_img.jpg\) launch binder](#)

If binder is too slow for you, you can view static html versions:

- <http://web.eecs.umich.edu/~fessler/demo/00-isbi.html>
- <http://web.eecs.umich.edu/~fessler/demo/01-odwt.html>

You can also view the notebook code directly:

- [demo/](#)



Simplified signal model:

$$\mathbf{s} = \mathbf{F}\mathbf{x}, \quad F_{ij} = \exp(-\imath 2\pi \vec{\nu}_i \cdot \vec{r}_j)$$

- $\mathbf{s} \in \mathbb{C}^M$ signal samples recorded by an ideal MR receive coil
- $\mathbf{x} \in \mathbb{C}^N$ discretized version of the transverse magnetization
- $\vec{\nu}_i$ k-space sample location of the i th sample (units cycles/cm)
- \vec{r}_j spatial coordinates of the center of the j th pixel (units cm)
- $\mathbf{F} \in \mathbb{C}^{M \times N}$ Fourier encoding matrix

For Cartesian sampling $\mathbf{s} = \mathbf{F}\mathbf{x} = \text{fft}(\mathbf{x})$ and $\mathbf{F}^{-1} \mathbf{s} = \frac{1}{N} \mathbf{F}' \mathbf{s} = \text{ifft}(\mathbf{s})$

Prevalent in clinical MRI

Reconstruction is “interesting” when considering

- non-Cartesian sampling [56],
- “accelerated” scanning with $M < N$ samples [16, 35],
- non-Fourier effects like magnetic field inhomogeneity [57],
- multiple receive coils.

$$\mathbf{y}_l = \mathbf{s}_l + \boldsymbol{\varepsilon}_l, \quad \mathbf{s}_l = \mathbf{F} \mathbf{C}_l \mathbf{x} \quad l = 1, \dots, L$$

- $\mathbf{y}_l \in \mathbb{C}^M$: noisy samples recorded by the l th of L receive coils
 - \mathbf{C}_l : $N \times N$ diagonal matrix containing the l th coil sensitivity pattern.
- Combining yields a standard forward model in MRI:

$$\begin{bmatrix} \mathbf{y}_1 \\ \vdots \\ \mathbf{y}_L \end{bmatrix} = \mathbf{y} = \underbrace{(\mathbf{I}_L \otimes \mathbf{F})}_{\mathbf{A}} \mathbf{C} \mathbf{x} + \boldsymbol{\varepsilon}, \quad \mathbf{C} = \begin{bmatrix} \mathbf{C}_1 \\ \vdots \\ \mathbf{C}_L \end{bmatrix} \quad (1)$$

- $\mathbf{A} \in \mathbb{C}^{ML \times N}$: system matrix
- $\mathbf{y} \in \mathbb{C}^{ML}$: measured k-space data
- $\mathbf{x} \in \mathbb{C}^N$: latent image
- $\boldsymbol{\varepsilon}$: complex white Gaussian noise [58]

Extensions consider other physics effects like relaxation and field inhomogeneity [55].

Goal: recover image \mathbf{x} from data \mathbf{y}

Introduction

Brief review of classic methods (> 10 years old)

 Ordinary least-squares

 Smooth regularization

Sparsity regularizers: Basic

Sparsity regularizers: Advanced

Adaptive regularizers

Denoising-based “regularization”

Deep-learning approaches for image reconstruction

Looking forward

Bibliography

When $ML \geq N$, linear model (1) is over-determined so use ordinary least-squares:

$$\begin{aligned}\hat{\mathbf{x}} &= \arg \min_{\mathbf{x} \in \mathbb{C}^N} \frac{1}{2} \|\mathbf{Ax} - \mathbf{y}\|_2^2 = (\mathbf{A}'\mathbf{A})^{-1}\mathbf{A}'\mathbf{y} \\ &= \left(\sum_{I=1}^L \mathbf{C}_I' \mathbf{F}' \mathbf{F} \mathbf{C}_I \right)^{-1} \left(\sum_{I=1}^L \mathbf{C}_I' \mathbf{F}' \mathbf{y} \right). \quad (2)\end{aligned}$$

- For fully sampled Cartesian k-space data where $\mathbf{F}^{-1} = \frac{1}{N} \mathbf{F}'$, it simplifies to $\hat{\mathbf{x}} = \left(\sum_{I=1}^L \mathbf{C}_I' \mathbf{C}_I \right)^{-1} \left(\sum_{I=1}^L \mathbf{C}_I' \mathbf{F}^{-1} \mathbf{y} \right)$, optimal coil combination approach [13].
- For regularly under-sampled Cartesian data, $\mathbf{F}'\mathbf{F}$ has a simple block structure
 \implies SENSE reconstruction [16].

Regularization is essential for

- under-sampled problems ($ML < N$)
- poorly conditioned problems, e.g., non-Cartesian sampling

Simplest form is quadratically regularized LS (RLS):

$$\hat{\mathbf{x}} = \arg \min_{\mathbf{x} \in \mathbb{C}^N} \frac{1}{2} \|\mathbf{A}\mathbf{x} - \mathbf{y}\|_2^2 + \beta \frac{1}{2} \|\mathbf{T}\mathbf{x}\|_2^2, \quad (3)$$

- $\beta > 0$: regularization parameter
- \mathbf{T} : $K \times N$ matrix transform such as finite differences (spatial smoothness model).
 - ▶ The conjugate gradient (CG) algorithm is well-suited [17, 57]
 - ▶ The Hessian matrix $\mathbf{A}'\mathbf{A} + \beta \mathbf{T}'\mathbf{T}$ often is approximately Toeplitz [59]
 \implies CG with circulant preconditioning [60]
 - ▶ RLS is now passé, but CG often used as an inner step [61],
even in recent deep learning methods for MRI reconstruction [62]

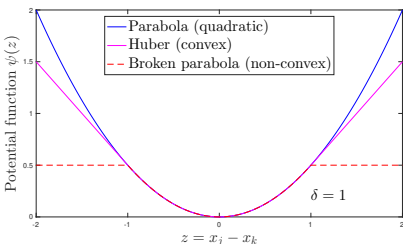
- ▶ Quadratic regularizer blurs edges when \mathbf{T} is finite differences.
- ▶ Edge-preserving regularizer reduces such blur:

$$\hat{\mathbf{x}} = \arg \min_{\mathbf{x} \in \mathbb{C}^N} \frac{1}{2} \|\mathbf{Ax} - \mathbf{y}\|_2^2 + \beta \psi(\mathbf{Tx}). \quad (4)$$

ψ : nonquadratic potential function,
typically convex and smooth

Huber function [63], hyperbola [64, 65],

Fair potential $\psi(z) = \delta^2 (|z/\delta| - \log(1 + |z/\delta|))$

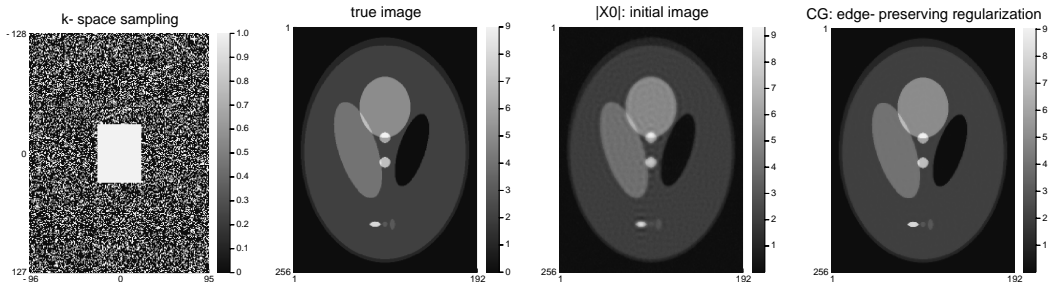


- ▶ Roots in Bayesian methods for Markov random fields [66, 67]

Algorithm options:

- ▶ Nonlinear CG algorithm
- ▶ 3MG (majorize-minimize memory gradient) algorithm [65]
- ▶ optimized gradient method (OGM) [68]
 - optimal worst-case first-order method for convex cost functions with Lipschitz continuous gradients [69]
 - OGM convergence rate bound $2\times$ better than Nesterov's fast gradient method [70]
- ▶ line-search OGM [71].

Edge-preserving regularization: example



ψ : Fair potential, $\delta = 0.1$

T : finite differences

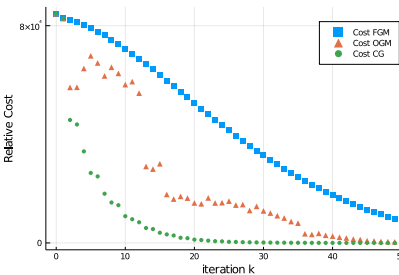
= corner-rounded TV

Demo notebook: [01-recon](#)

<https://github.com/JeffFessler/mirt-demo>

Final NRMSE: 1.55%

(Cost function is locally strongly convex.)



Introduction

Brief review of classic methods (> 10 years old)

Sparsity regularizers: Basic

Sparsity models: synthesis form

Proximal methods: ISTA/FISTA/POGM

Sparsity models: analysis form

Sparsity regularizers: Advanced

Adaptive regularizers

Denoising-based “regularization”

Deep-learning approaches for image reconstruction

Looking forward

Bibliography

Received: 1 January 2020

Revised: 28 April 2020

Accepted: 30 April 2020

DOI: 10.1002/mrm.28338

FULL PAPER

Magnetic Resonance in Medicine

Advancing machine learning for MR image reconstruction with an open competition: Overview of the 2019 fastMRI challenge

Florian Knoll¹  | Tullie Murrell² | Anuroop Sriram² | Nafissa Yakubova² |
Jure Zbontar² | Michael Rabbat² | Aaron Defazio² | Matthew J. Muckley¹  |
Daniel K. Sodickson¹ | C. Lawrence Zitnick² | Michael P. Recht¹

“the winners ... chose approaches that used a combination of a learned prior and a data-fidelity term that encodes information about the MR physics of the acquisition, in line with approaches that can be seen as neural network extensions of classic iterative image reconstruction methods” [72]

► **Synthesis model:**

Assume $\mathbf{x} = \mathbf{B}\mathbf{z}$

\mathbf{B} : $N \times K$ matrix (“basis”), usually wide (over complete)

$\mathbf{z} \in \mathbb{C}^K$ **sparse** coefficient vector

\implies use $\|\mathbf{z}\|_1$

► **Analysis model:**

Assumes $\mathbf{T}\mathbf{x}$ is **sparse**

\mathbf{T} : $K \times N$ transformation matrix, usually tall

\implies use $\|\mathbf{T}\mathbf{x}\|_1$

Most likely used in recent FDA-approved CS methods.

► Equivalent if $\mathbf{B} = \mathbf{T}^{-1}$ (but usually both are non-square)

► optimization trade-off: $\|\mathbf{z}\|_1$ is easier than $\|\mathbf{T}\mathbf{x}\|_1$, but $K > N$

All models are wrong, but some models are useful...

- ▶ Typical compressed sensing cost function for a synthesis model:

$$\hat{\mathbf{x}} = \mathbf{B}\hat{\mathbf{z}}, \quad \hat{\mathbf{z}} = \arg \min_{\mathbf{z} \in \mathbb{C}^K} \frac{1}{2} \|\mathbf{A}\mathbf{B}\mathbf{z} - \mathbf{y}\|_2^2 + \beta \|\mathbf{z}\|_1 \quad (5)$$

- ▶ 1-norm is convex relaxation of the ℓ_0 counting measure encourages coefficients $\hat{\mathbf{z}}$ to be sparse.
- ▶ Also known as the LASSO problem [73, 74]
- ▶ Numerous optimization algorithms
proximal optimized gradient method (POGM) particularly effective
(Taylor et al., 2017) [75, 76]

Introduction

Brief review of classic methods (> 10 years old)

Sparsity regularizers: Basic

Sparsity models: synthesis form

Proximal methods: ISTA/FISTA/POGM

Sparsity models: analysis form

Sparsity regularizers: Advanced

Adaptive regularizers

Denoising-based “regularization”

Deep-learning approaches for image reconstruction

Looking forward

Bibliography

- ▶ Classical approach: iterative soft thresholding algorithm (ISTA) [77]
aka proximal gradient method (PGM) and proximal forward-backward splitting [78],

$$\mathbf{z}_{k+1} = \text{soft}\left(\mathbf{z}_k - \mathbf{D}^{-1} \mathbf{B}' \mathbf{A}' (\mathbf{A} \mathbf{B} \mathbf{z}_k - \mathbf{y}), \beta / \mathbf{d}\right), \quad (6)$$

- soft thresholding : $\text{soft}(z, c) = \text{sign}(z) \max(|z| - c, 0)$
- $\mathbf{D} = \text{Diag}\{\mathbf{d}\}$: diagonal matrix satisfying $\mathbf{D} \succeq \mathbf{B}' \mathbf{A}' \mathbf{A} \mathbf{B}$ [79]

Slight generalization of usual ISTA where $\mathbf{D} = L\mathbf{I}$ and $L = \|\mathbf{B}' \mathbf{A}' \mathbf{A} \mathbf{B}\|_2$.

- ▶ $O(1/k)$ convergence bound of ISTA is undesirably slow
- ▶ fast iterative soft thresholding algorithm (FISTA) [80, 81], has $O(1/k^2)$ bound
aka fast proximal gradient method (FPGM)

Composite cost function:

$$\hat{\mathbf{x}} = \arg \min_{\mathbf{x}} \underbrace{f(\mathbf{x})}_{\text{smooth}} + \underbrace{g(\mathbf{x})}_{\text{prox friendly}}$$

- ▶ Recent extension: proximal optimized gradient method (POGM)
- ▶ worst-case convergence bound about $2\times$ better than FISTA/FPGM [75, 76].
- ▶ ISTA / FISTA / POGM nearly equally simple to implement
equivalent computation time per iteration, dominated by ∇f and prox_g
- ▶ POGM converges faster than FISTA empirically [82, 83, 84, 85],
when combined with adaptive restart [86, 76].
- ▶ Active research area [87, 88, 85]

Initialize $\mathbf{w}_0 = \mathbf{x}_0$, $\theta_0 = 1$. Then for $k = 1 : N$:

$$\theta_k = \begin{cases} \frac{1}{2} \left(1 + \sqrt{4\theta_{k-1}^2 + 1} \right), & k < N \\ \frac{1}{2} \left(1 + \sqrt{8\theta_{k-1}^2 + 1} \right), & k = N \end{cases} \quad \gamma_k = \frac{1}{L} \frac{2\theta_{k-1} + \theta_k - 1}{\theta_k}$$

$$\mathbf{w}_k = \mathbf{x}_{k-1} - \frac{1}{L} \nabla f(\mathbf{x}_{k-1})$$

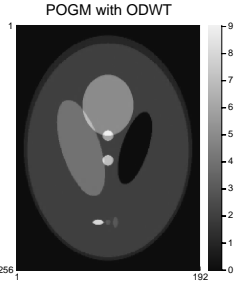
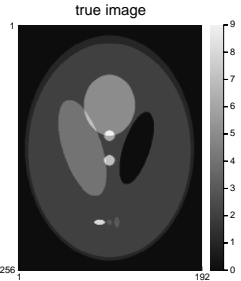
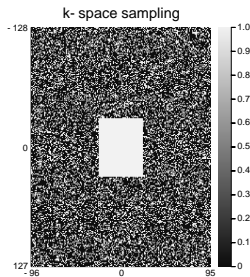
$$\mathbf{z}_k = \mathbf{w}_k + \frac{\theta_{k-1} - 1}{\theta_k} (\mathbf{w}_k - \mathbf{w}_{k-1}) + \frac{\theta_{k-1}}{\theta_k} (\mathbf{w}_k - \mathbf{x}_{k-1}) + \frac{\theta_{k-1} - 1}{L\gamma_{k-1}\theta_k} (\mathbf{z}_{k-1} - \mathbf{x}_{k-1})$$

$$\mathbf{x}_k = \text{prox}_{\gamma_k g}(\mathbf{z}_k) = \arg \min_{\mathbf{x}} \frac{1}{2} \|\mathbf{x} - \mathbf{z}_k\|_2^2 + \gamma_k g(\mathbf{x})$$

POGM method [75] for minimizing $f(\mathbf{x}) + g(\mathbf{x})$ where f is convex with L -Lipschitz smooth gradient and g is convex. See [76] for adaptive restart version.

POGM illustrated

J. Fessler
Recon



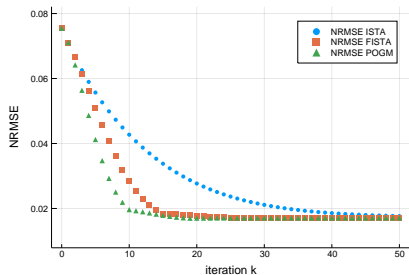
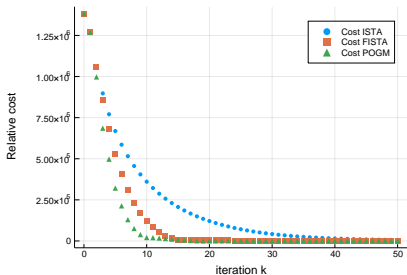
Demo:

01-recon

B: ODWT

Final NRMSE:

1.71%



- ▶ Typical optimization problem for analysis sparsity model:

$$\hat{\mathbf{x}} = \arg \min_{\mathbf{x}} \frac{1}{2} \|\mathbf{Ax} - \mathbf{y}\|_2^2 + \beta \|\mathbf{T}\mathbf{x}\|_1 \quad (7)$$

\mathbf{T} : sparsifying operator

- wavelet transform
- finite differences, aka total variation (TV) [33]
- both [38]

- ▶ FDA-approved methods for compressed sensing MRI presumably related to (7).
- ▶ The analysis optimization problem (7) is harder than the synthesis form (5) due to the matrix \mathbf{T} within 1-norm.

PGM for analysis regularizer problem (7):

$$\begin{aligned}\tilde{\mathbf{x}}_k &\triangleq \mathbf{x}_k - \frac{1}{L} \mathbf{A}' (\mathbf{A}\mathbf{x}_k - \mathbf{y}) \quad (\text{gradient step}) \\ \mathbf{x}_{k+1} &= \arg \min_{\mathbf{x}} \frac{L}{2} \|\mathbf{x} - \tilde{\mathbf{x}}_k\|_2^2 + \beta \|\mathbf{T}\mathbf{x}\|_1 = \text{prox}_{\frac{\beta}{L} \|\mathbf{T}\cdot\|_1}(\tilde{\mathbf{x}}_k)\end{aligned}\tag{8}$$

$L = \|\mathbf{A}\|_2^2$: Lipschitz constant

- ▶ No simple solution for the proximity operator
- ▶ Inner iterative methods are required, typically involving dual formulations [89, 81]
- ▶ Perhaps main drawback of analysis regularization
- ▶ \implies PGM / FPGM / POGM less attractive for (7)

Circumventing the challenge of the matrix \mathbf{T} in the 1-norm:

► Corner rounding

Use smooth approximation: $|z| \approx \sqrt{|z|^2 + \epsilon}$

- Akin to edge-preserving regularization
- Proximal operators have no thresholding effect that induces sparsity

► Penalty approach

Replace (7) with the following alternative [90]:

$$\hat{\mathbf{x}} = \arg \min_{\mathbf{x}} \frac{1}{2} \|\mathbf{Ax} - \mathbf{y}\|_2^2 + \beta R_\alpha(\mathbf{x}), \quad R_\alpha(\mathbf{x}) = \min_{\mathbf{z}} \frac{1}{2} \|\mathbf{T}\mathbf{x} - \mathbf{z}\|_2^2 + \alpha \|\mathbf{z}\|_1.$$

- Fact: $R_\alpha(\mathbf{x}) = \psi(\mathbf{T}\mathbf{x}, \alpha)$ where ψ is the Huber function \implies corner rounding
- Requires choosing parameter α .

► Iterative reweighted least-squares (FOCUSS) [36], akin to corner rounding

Replace $\|T\mathbf{x}\|_1$ in (7) with exactly equivalent constrained minimization problem involving auxiliary variable(s):

$$\hat{\mathbf{x}} = \arg \min_{\mathbf{x}} \min_{\mathbf{z} : \mathbf{z} = T\mathbf{x}} \frac{1}{2} \|\mathbf{A}\mathbf{x} - \mathbf{y}\|_2^2 + \beta \|\mathbf{z}\|_1. \quad (9)$$

- split Bregman algorithm [91]
- augmented Lagrangian (AL) methods [92, 61]
- alternating direction multiplier method (ADMM) [93, 94]
- Douglas-Rachford splitting method

Corresponding **augmented Lagrangian** for constrained problem for (9):

$$L(\mathbf{x}, \mathbf{z}; \gamma, \mu) = \frac{1}{2} \|\mathbf{Ax} - \mathbf{y}\|_2^2 + \beta \|\mathbf{z}\|_1 + \text{real}\{\langle \gamma, \mathbf{T}\mathbf{x} - \mathbf{z} \rangle\} + \frac{\mu}{2} \|\mathbf{T}\mathbf{x} - \mathbf{z}\|_2^2,$$

$\gamma \in \mathbb{C}^K$: Lagrange multipliers

$\mu > 0$: AL penalty parameter (affects the convergence rate, not $\hat{\mathbf{x}}$)

Scaled dual variable: $\boldsymbol{\eta} \triangleq (1/\mu)\gamma \implies$ scaled augmented Lagrangian:

$$L(\mathbf{x}, \mathbf{z}; \boldsymbol{\eta}, \mu) = \frac{1}{2} \|\mathbf{Ax} - \mathbf{y}\|_2^2 + \beta \|\mathbf{z}\|_1 + \frac{\mu}{2} \left(\|\mathbf{T}\mathbf{x} - \mathbf{z} + \boldsymbol{\eta}\|_2^2 - \|\boldsymbol{\eta}\|_2^2 \right).$$

AL approach alternates between

- descent updates of primal variables \mathbf{x}, \mathbf{z} ,
- ascent update of scaled dual variable $\boldsymbol{\eta}$.

$$L(\mathbf{x}, \mathbf{z}; \boldsymbol{\eta}, \mu) = \frac{1}{2} \|\mathbf{Ax} - \mathbf{y}\|_2^2 + \beta \|\mathbf{z}\|_1 + \frac{\mu}{2} (\|\mathbf{Tx} - \mathbf{z} + \boldsymbol{\eta}\|_2^2 - \|\boldsymbol{\eta}\|_2^2).$$

\mathbf{z} update is simply soft thresholding:

$$\mathbf{z}_{k+1} = \text{soft}(\mathbf{T}\mathbf{x}_k + \boldsymbol{\eta}_k, \beta/\mu).$$

\mathbf{x} update minimizes a quadratic function (use PCG):

$$\mathbf{x}_{k+1} = (\mathbf{A}'\mathbf{A} + \mu \mathbf{T}'\mathbf{T})^{-1}(\mathbf{A}'\mathbf{y} + \mu \mathbf{T}'(\mathbf{z}_{k+1} - \boldsymbol{\eta}_k)).$$

$\boldsymbol{\eta}$ update is ascent:

$$\boldsymbol{\eta}_{k+1} = \boldsymbol{\eta}_k + (\mathbf{T}\mathbf{x}_{k+1} - \mathbf{z}_{k+1}).$$

- Adaptive methods for tuning μ [94, 95, 96].
- Parallel ADMM updates are also possible [97, 98].

Properties of $\mathbf{A} = \mathbf{F}_L \mathbf{C}$, $\mathbf{F}_L \triangleq \mathbf{I}_L \otimes \mathbf{F}$:

$\mathbf{F}'\mathbf{F}$: circulant (for Cartesian sampling) or Toeplitz (for non-Cartesian sampling)

\mathbf{C}_I : diagonal coil sensitivity matrix

Alternative variable split with simpler updates [61]:

$$\hat{\mathbf{x}} = \arg \min_{\mathbf{x} \in \mathbb{C}^N} \min_{\mathbf{u} \in \mathbb{C}^{NL}: \mathbf{u} = \mathbf{Cx}} \min_{\mathbf{z} \in \mathbb{C}^K: \mathbf{z} = \mathbf{Tv}} \min_{\mathbf{v} \in \mathbb{C}^N: \mathbf{v} = \mathbf{x}} \frac{1}{2} \|\mathbf{F}_L \mathbf{u} - \mathbf{y}\|_2^2 + \beta \|\mathbf{z}\|_1, \quad (10)$$

\mathbf{z} update : soft thresholding

\mathbf{x} update : involves diagonal matrix $\mathbf{C}'\mathbf{C}$

\mathbf{v} update : involves $\mathbf{T}'\mathbf{T}$ that is circulant or Toeplitz \Rightarrow use FFT or DCT

\mathbf{u} update : involves $\mathbf{F}'_L \mathbf{F}_L$ that is circulant or Toeplitz.

- Primary drawback: more AL penalty parameters; (condition number criteria can help [61]).
- Many variations, e.g., [98] [99].

A key idea behind duality-based methods:

$$\|\mathbf{T}\mathbf{x}\|_1 = \max_{\mathbf{z} \in \mathcal{Z}} \text{real}\{\langle \mathbf{z}, \mathbf{T}\mathbf{x} \rangle\}, \quad \mathcal{Z} \triangleq \left\{ \mathbf{z} \in \mathbb{C}^K : \|\mathbf{z}\|_\infty \leq 1 \right\}.$$

Thus the analysis regularized problem (7) is equivalent to constrained problem:

$$\arg \min_{\mathbf{x}} \max_{\mathbf{z} \in \mathcal{Z}} \frac{1}{2} \|\mathbf{A}\mathbf{x} - \mathbf{y}\|_2^2 + \beta \text{real}\{\langle \mathbf{z}, \mathbf{T}\mathbf{x} \rangle\}. \quad (11)$$

Primal-dual methods typically alternate between updating primal variable \mathbf{x} and dual variable \mathbf{z} , using more convenient alternatives to (11).

- Separate multiplication by \mathbf{A} and by \mathbf{A}' without requiring inner CG iterations.
- Convergence guarantees and $O(1/k^2)$ rates [100, 101, 99, 102, 103, 104, 105, 106, 107].
- Require running a power iteration to find a Lipschitz constant.
- Like AL methods, have algorithm parameters to tune for convergence rate.

Introduction

Brief review of classic methods (> 10 years old)

Sparsity regularizers: Basic

Sparsity regularizers: Advanced

- Non-SENSE methods

- Patch-based sparsity models

- Convolutional regularizers

Adaptive regularizers

Denoising-based “regularization”

Deep-learning approaches for image reconstruction

Looking forward

Bibliography

Introduction

Brief review of classic methods (> 10 years old)

Sparsity regularizers: Basic

Sparsity regularizers: Advanced

Non-SENSE methods

GRAPPA methods

Calibrationless methods

Patch-based sparsity models

Convolutional regularizers

Adaptive regularizers

Denoising-based “regularization”

Deep-learning approaches for image reconstruction

Looking forward

Bibliography

Instead of a single latent image \mathbf{x} , define a latent image for each coil $\mathbf{x}_l \triangleq \mathbf{C}_l \mathbf{x}$.

Measurement model: $\mathbf{y}_l = \mathbf{F} \mathbf{x}_l + \boldsymbol{\epsilon}_l$.

Reconstruct L images $\mathbf{X} = [\mathbf{x}_1 \dots \mathbf{x}_L]$ from measurements $\mathbf{Y} = [\mathbf{y}_1 \dots \mathbf{y}_L] \in \mathbb{C}^{M \times L}$.

Account for some relationships between those L images.

Multiplication by the smooth sensitivity map \mathbf{C}_l in the image domain

⇒ convolution with a small kernel in the frequency domain

⇒ any point in k-space ≈ a linear combination of its neighbors

⇒ GRAPPA consistency condition [18] $\text{vec}(\mathbf{X}) \approx \mathbf{G} \text{vec}(\mathbf{X})$

\mathbf{G} involves small k-space kernels learned from calibration k-space data

“SPIRiT” [108] optimization problems like:

$$\hat{\mathbf{X}} = \arg \min_{\mathbf{X} \in \mathbb{C}^{N \times L}} \frac{1}{2} \| \mathbf{F} \mathbf{X} - \mathbf{Y} \|_{\text{Frob}}^2 + \beta_1 \frac{1}{2} \| (\mathbf{G} - \mathbf{I}) \text{vec}(\mathbf{X}) \|_2^2 + \beta_2 R(\mathbf{X}),$$

$R(\mathbf{X})$: regularizer that encourages joint image sparsity [109].

Needs no sensitivity maps; use CG [108] or ADMM [110, 111].

Subspace and joint sparsity approaches go further by circumventing finding the calibration matrix \mathbf{G} [112, 45, 46, 113]

Introduction

Brief review of classic methods (> 10 years old)

Sparsity regularizers: Basic

Sparsity regularizers: Advanced

- Non-SENSE methods

- Patch-based sparsity models

- Convolutional regularizers

Adaptive regularizers

Denoising-based “regularization”

Deep-learning approaches for image reconstruction

Looking forward

Bibliography

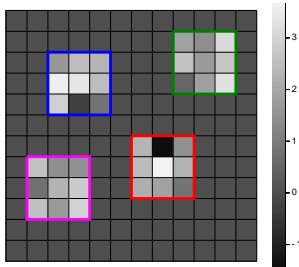
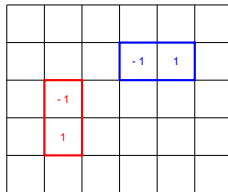
Using TV regularizer $R(\mathbf{x}) = \|\mathbf{T}\mathbf{x}\|_1$
where \mathbf{T} is finite-differences
 \equiv patches of size 2×1 .

Larger patches provide more context
for distinguishing signal from noise.

cf. CNN approaches

Patch-based regularizers:

- synthesis models
- analysis methods

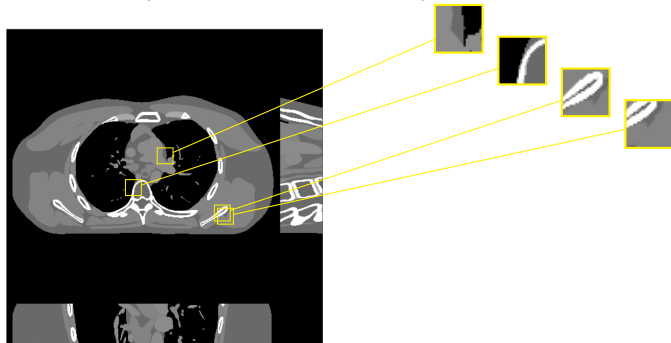


Assumption: if \mathbf{x} is a plausible image, then each patch has

$$\mathbf{P}_p \mathbf{x} \approx \mathbf{Dz}_p,$$

for a sparse coefficient vector \mathbf{z}_p . (Synthesis approach.)

- ▶ $\mathbf{P}_p \mathbf{x}$ extracts the p th of P patches from \mathbf{x}
- ▶ \mathbf{D} is a (typically overcomplete) dictionary for patches



Patch synthesis model uses sparse linear combination of patch atoms: $\mathbf{P}_p \mathbf{x} \approx \mathbf{Dz}_p$

$\mathbf{P}_p \in \{0, 1\}^{d \times N}$: extracts p th of P d -pixel patches from image \mathbf{x}

$\mathbf{D} \in \mathbb{C}^{d \times J}$: dictionary of J patch atoms

$\mathbf{z}_p \in \mathbb{C}^J$: sparse coefficient vector for p th patch.

Natural regularizer for patch synthesis sparsity model [114]:

$$\hat{\mathbf{x}} = \arg \min_{\mathbf{x}} \frac{1}{2} \|\mathbf{Ax} - \mathbf{y}\|_2^2 + \beta R(\mathbf{x}), \quad R(\mathbf{x}) = \min_{\{\mathbf{z}_p\}} \sum_{p=1}^P \frac{1}{2} \|\mathbf{P}_p \mathbf{x} - \mathbf{Dz}_p\|_2^2 + \alpha \|\mathbf{z}_p\|_1.$$

Use **alternating minimization** algorithms for optimization:

- \mathbf{x} update is quadratic (PCG),
- \mathbf{z}_p update is sparse coding (POGM).
- Basic approach would require storing JN coefficient values $\{\mathbf{z}_p\}$.

Patch analysis model assumes: $\mathbf{T}\mathbf{P}_p\mathbf{x}$ tends to be sparse

$\mathbf{P}_p \in \{0, 1\}^{d \times N}$: extracts p th of P d -pixel patches from image \mathbf{x}

$\mathbf{T} \in \mathbb{C}^{K \times d}$: patch sparsifying transform (e.g., DCT)

Natural regularizer for patch analysis sparsity model [115]:

$$\hat{\mathbf{x}} = \arg \min_{\mathbf{x}} \frac{1}{2} \|\mathbf{A}\mathbf{x} - \mathbf{y}\|_2^2 + \beta R(\mathbf{x}), \quad R(\mathbf{x}) = \min_{\{\mathbf{z}_p\}} \sum_{p=1}^P \frac{1}{2} \|\mathbf{T}\mathbf{P}_p\mathbf{x} - \mathbf{z}_p\|_2^2 + \alpha \|\mathbf{z}_p\|_1.$$

Use **alternating minimization** algorithms for optimization:

- \mathbf{x} update is quadratic (PCG),
Hessian w.r.t. \mathbf{x} : $\mathbf{A}'\mathbf{A} + \beta \sum_p \mathbf{P}'_p \mathbf{T}' \mathbf{T}\mathbf{P}_p$, simplifies when \mathbf{T} is unitary
- \mathbf{z}_p update is simply soft thresholding (easier than sparse coding!)
- Efficient implementation uses accumulator: $\tilde{\mathbf{x}}_t \triangleq \sum_{p=1}^P \mathbf{P}'_p \mathbf{T}' \text{soft}(\mathbf{T}\mathbf{P}_p\mathbf{x}_t, \alpha)$,
avoids storing all KN coefficient values $\{\mathbf{z}_p\}$.

Patch analysis sparsity formulation reiterated:

$$\hat{\mathbf{x}} = \arg \min_{\mathbf{x}} \frac{1}{2} \|\mathbf{Ax} - \mathbf{y}\|_2^2 + \beta R(\mathbf{x}), \quad R(\mathbf{x}) = \min_{\{\mathbf{z}_p\}} \sum_{p=1}^P \frac{1}{2} \|\mathbf{TP}_p \mathbf{x} - \mathbf{z}_p\|_2^2 + \alpha \|\mathbf{z}_p\|_1.$$

Alternating minimization, aka two-block **block coordinate descent (BCD)**:

- \mathbf{x} update : quadratic
- \mathbf{z}_p update : soft thresholding of transform coefficients

Combining:

$$\tilde{\mathbf{x}}_t = \sum_{p=1}^P \mathbf{P}'_p \mathbf{T}' \text{soft}(\mathbf{TP}_p \mathbf{x}_t, \alpha) \quad \text{denoising, makes "prior"}$$

$$\mathbf{x}_{t+1} = \arg \min_{\mathbf{x}} \frac{1}{2} \|\mathbf{Ax} - \mathbf{y}\|_2^2 + \beta \frac{1}{2} \|\mathbf{x} - \tilde{\mathbf{x}}_t\|_2^2 \quad \text{physics / k-space data.}$$

Cost function decreases monotonically here

May replace denoising step with NLM, BM3D, CNN, ...

Introduction

Brief review of classic methods (> 10 years old)

Sparsity regularizers: Basic

Sparsity regularizers: Advanced

Non-SENSE methods

Patch-based sparsity models

Convolutional regularizers

Adaptive regularizers

Denoising-based “regularization”

Deep-learning approaches for image reconstruction

Looking forward

Bibliography

Close relative of patch models is convolutional sparsity models [116, 117, 118].

Convolutional synthesis model assumes $\mathbf{x} \approx \sum_{k=1}^K \mathbf{h}_k * \mathbf{z}_k$

- \mathbf{h}_k : filters (typically learned from training data) [119]
- \mathbf{z}_k : sparse coefficient images (requires NK storage, challenging in 3D or dynamic)

Corresponding regularizer :

$$\hat{\mathbf{x}} = \arg \min_{\mathbf{x}} \frac{1}{2} \|\mathbf{A}\mathbf{x} - \mathbf{y}\|_2^2 + \beta R(\mathbf{x}), \quad R(\mathbf{x}) = \min_{\{\mathbf{z}_k\}} \frac{1}{2} \left\| \mathbf{x} - \sum_{k=1}^K \mathbf{h}_k * \mathbf{z}_k \right\|_2^2 + \alpha \|\mathbf{z}_k\|_1.$$

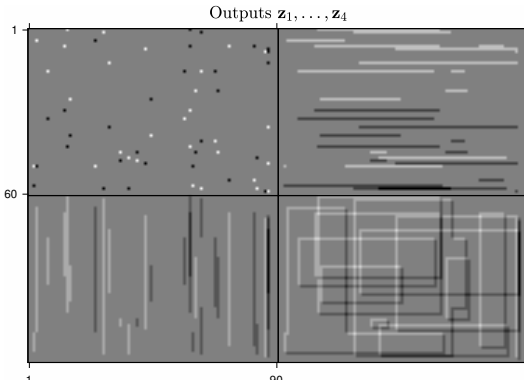
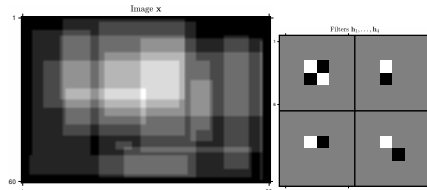
Use **alternating minimization**:

- \mathbf{x} update : quadratic (PCG)
- \mathbf{z}_k update : sparse coding (POGM)

Assumption: For a plausible image \mathbf{x} , the filter outputs $\{\mathbf{h}_k * \mathbf{x}\}$ are sparse, for some filters $\{\mathbf{h}_k\}_{k=1}^K$ [117]

- ▶ For more plausible images, the outputs $\{\mathbf{h}_k * \mathbf{x}\}$ are more sparse.
- ▶ $*$ denotes convolution
- ▶ Inherently shift invariant and no patches

Example (hand crafted filters):



Convolution analysis model assumes $\mathbf{h}_k * \mathbf{x}$ is sparse. Corresponding regularizer:

$$\hat{\mathbf{x}} = \arg \min_{\mathbf{x}} \frac{1}{2} \|\mathbf{A}\mathbf{x} - \mathbf{y}\|_2^2 + \beta R(\mathbf{x}), \quad R(\mathbf{x}) = \min_{\{\mathbf{z}_k\}} \sum_{k=1}^K \frac{1}{2} \|\mathbf{h}_k * \mathbf{x} - \mathbf{z}_k\|_2^2 + \alpha \|\mathbf{z}_k\|_1.$$

Use **alternating minimization** algorithm [116]:

- \mathbf{x} update : quadratic (GD or PCG),
- \mathbf{z}_k update : soft thresholding.
- Implement efficiently without storing NK sparse coefficients:

$$\tilde{\mathbf{x}}_t = \sum_{k=1}^K \mathbf{h}_k^{(-)} * \text{soft}(\mathbf{h}_k * \mathbf{x}_{t-1}) \quad (\text{denoising, accumulator})$$

$$\mathbf{x}_{t+1} = \arg \min_{\mathbf{x}} \frac{1}{2} \|\mathbf{A}\mathbf{x} - \mathbf{y}\|_2^2 + \beta \frac{1}{2} \|\mathbf{x} - \tilde{\mathbf{x}}_t\|_2^2 \quad (\text{physics})$$

Image models / cost functions:

- ▶ Image sparse synthesis (e.g., wavelet basis)
- ▶ Image transform/analysis sparsity
(e.g., finite differences for total variation, wavelets, ...)
- ▶ Patch dictionary sparsity
- ▶ Patch transform sparsity
- ▶ Convolutional sparsity

Algorithm components:

- ▶ gradient-based (CG)
- ▶ proximal operations (soft/d thresholding)
- ▶ alternating minimization
- ▶ duality (AL, ADMM, primal-dual, ...)

Introduction

Brief review of classic methods (> 10 years old)

Sparsity regularizers: Basic

Sparsity regularizers: Advanced

Adaptive regularizers

Population adaptive regularization

Patient adaptive regularization

Denoising-based “regularization”

Deep-learning approaches for image reconstruction

Looking forward

Bibliography

- ▶ Key required component for sparsity models:
 - ▶ D dictionary for patch-based synthesis model
 - ▶ T transform for patch-based analysis model
 - ▶ $\{h_k\}$ filters for convolutional models
- ▶ Options:
 - ▶ Hand-crafted mathematical models, e.g., discrete cosine transform (DCT)
 - ▶ Population adaptive approach:
learn model from “good quality” (e.g., fully sampled) representative training data
 - ▶ Patient adaptive (“blind”) approach:
adapt model for each patient by jointly optimizing image x ,
sparse coefficients Z and model component (D or T or $\{h_k\}$) [114, 115]
 - ▶ Hybrids of population and patient adaptive approaches [120]
- ▶ For adaptive schemes, constraints on the learned components are essential.

June 2018 special issue of IEEE Trans. on Medical Imaging [121]:



IEEE TRANSACTIONS ON MEDICAL IMAGING, VOL. 37, NO. 6, JUNE 2018

1289

Image Reconstruction Is a New Frontier of Machine Learning

Ge Wang^{ID}, Fellow, IEEE, Jong Chu Ye^{ID}, Senior Member, IEEE, Klaus Mueller^{ID}, Senior Member, IEEE,
and Jeffrey A. Fessler^{ID}, Fellow, IEEE



Properties of a convex regularizer



When learning the regularizer, convex functions allow most theory and avoid local minima!

In the interpretation $R(u) = -\log(p(u))$, a convex regularizer makes no sense for images!

0.5



+0.5



=



$$\frac{1}{2}R(u_1) + \frac{1}{2}R(u_2) \overset{\bullet}{\geq} R\left(\frac{1}{2}u_1 + \frac{1}{2}u_2\right)$$

Needs to have
lower $R(u)$ than one of
the other images!



- ▶ Data
 - ▶ Population adaptive methods
 - ▶ Patient adaptive methods (e.g., dynamic MRI?)
- ▶ Spatial structure
 - ▶ Patch-based models
 - ▶ Convolutional models
- ▶ Regularizer formulation
 - ▶ Synthesis (dictionary) approach
 - ▶ Analysis (sparsifying transforms) approach

Many options...

Introduction

Brief review of classic methods (> 10 years old)

Sparsity regularizers: Basic

Sparsity regularizers: Advanced

Adaptive regularizers

Population adaptive regularization

Example: learned transform

Patient adaptive regularization

Denoising-based “regularization”

Deep-learning approaches for image reconstruction

Looking forward

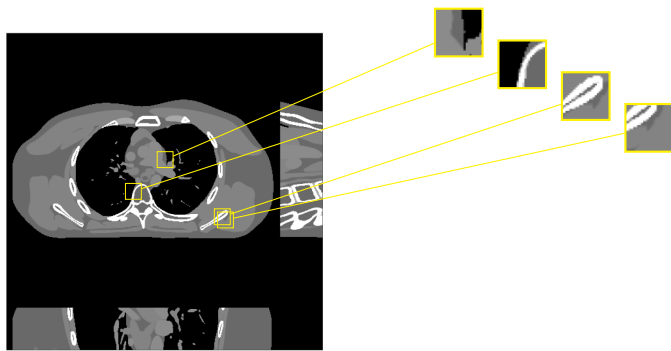
Bibliography

- ▶ Data
 - ▶ Population adaptive methods
 - ▶ Patient adaptive methods
- ▶ Spatial structure
 - ▶ Patch-based models
 - ▶ Convolutional models
- ▶ Regularizer formulation
 - ▶ Synthesis (dictionary) approach
 - ▶ Analysis (sparsifying transform) approach

Assumption: if \mathbf{x} is a plausible image, then each patch transform $\mathbf{T}\mathbf{P}_m\mathbf{x}$ is sparse.

- ▶ $\mathbf{P}_m\mathbf{x}$ extracts the m th of M patches from \mathbf{x}
- ▶ \mathbf{T} is a (often square) sparsifying transform matrix.

What \mathbf{T} ?



Given training images $\mathbf{x}_1, \dots, \mathbf{x}_L$ from a representative population, find transform \mathbf{T}_* that best sparsifies their patches:

$$\mathbf{T}_* = \arg \min_{\substack{\mathbf{T} \text{ unitary} \\ \{\mathbf{z}_{l,m}\}}} \sum_{l=1}^L \sum_{m=1}^M \|\mathbf{T}\mathbf{P}_m \mathbf{x}_l - \mathbf{z}_{l,m}\|_2^2 + \alpha \|\mathbf{z}_{l,m}\|_0$$

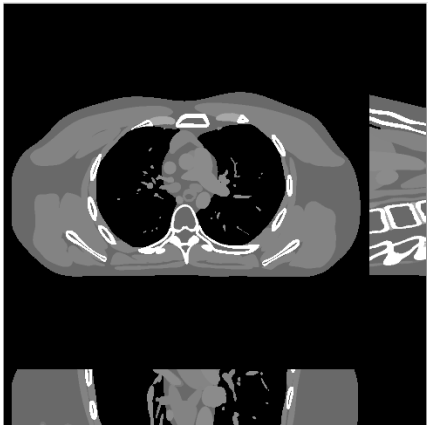
- ▶ Encourage aggregate sparsity, not patch-wise sparsity (cf K-SVD [122])
- ▶ Non-convex due to unitary constraint and $\|\cdot\|_0$
- ▶ Efficient alternating minimization algorithm [123]
 - \mathbf{z} update : simple hard thresholding
 - \mathbf{T} update : orthogonal Procrustes problem (SVD)
 - Subsequence convergence guarantees [123]

Example of learned sparsifying transform

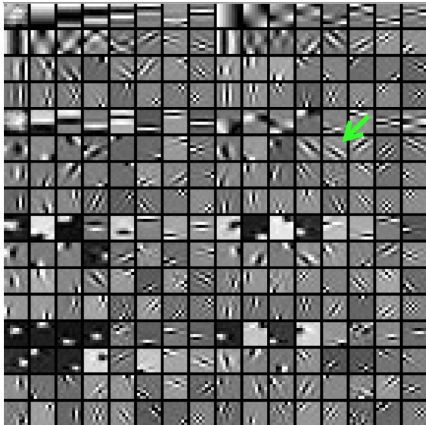
J. Fessler
Recon



3D X-ray training data



Parts of learned sparsifier T_*



(2D slices in x-y, x-z, y-z, from 3D image volume)

$8 \times 8 \times 8$ patches $\implies T_*$ is $8^3 \times 8^3 = 512 \times 512$

top 8×8 slice of 256 of the 512 rows of $T_* \uparrow_{59/123}$

Regularized inverse problem [124]:

$$\hat{\mathbf{x}} = \arg \min_{\mathbf{x}} \|\mathbf{A}\mathbf{x} - \mathbf{y}\|_2^2 + \beta R(\mathbf{x})$$

$$R(\mathbf{x}) = \min_{\{\mathbf{z}_m\}} \sum_{m=1}^M \|\mathbf{T}_* \mathbf{P}_m \mathbf{x} - \mathbf{z}_m\|_2^2 + \alpha \|\mathbf{z}_m\|_0.$$

\mathbf{T}_* adapted to population training data

Alternating minimization optimizer:

- ▶ \mathbf{z}_m update : simple hard thresholding
- ▶ \mathbf{x} update : quadratic problem (many options)

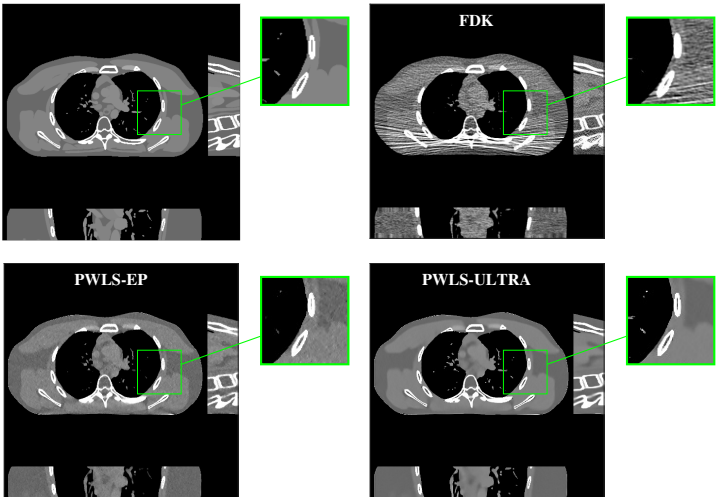
Linearized augmented Lagrangian method (LALM) [125]

Example: low-dose 3D X-ray CT simulation

J. Fessler
Recon

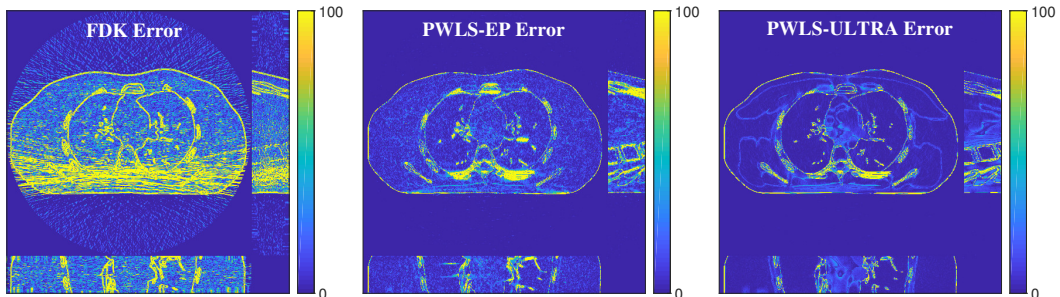


X. Zheng, S. Ravishankar,
Y. Long, JF:
IEEE T-MI, June 2018
[124].



3D X-ray CT simulation Error maps

J. Fessler
Recon



	X-ray Intensity	FDK	EP	ST T_*	ULTRA	ULTRA- $\{\tau_j\}$
RMSE in HU	1×10^4	67.8	34.6	32.1	30.7	29.2
	5×10^3	89.0	41.1	37.3	35.7	34.2

- ▶ Physics / statistics provides dramatic improvement
- ▶ Data adaptive regularization further reduces RMSE

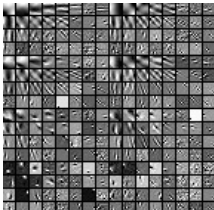
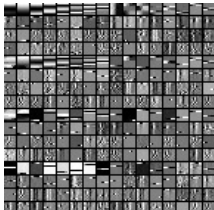
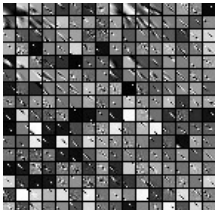
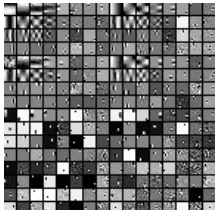
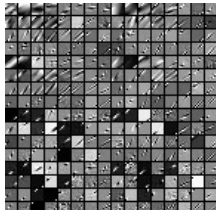
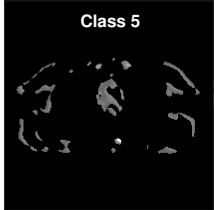
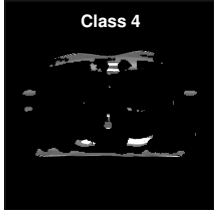
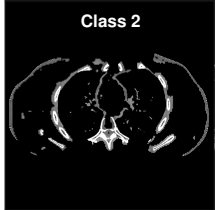
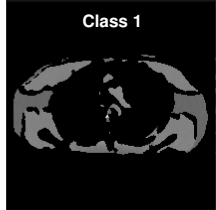
Given training images $\mathbf{x}_1, \dots, \mathbf{x}_L$ from a representative population, find a **set** of transforms $\{\hat{\mathbf{T}}_k\}_{k=1}^K$ that best sparsify image patches:

$$\{\hat{\mathbf{T}}_k\} = \arg \min_{\{\mathbf{T}_k \text{ unitary}\}} \min_{\{\mathbf{z}_{l,m}\}} \sum_{l=1}^L \sum_{m=1}^M \left(\min_{k \in \{1, \dots, K\}} \|\mathbf{T}_k \mathbf{P}_m \mathbf{x}_l - \mathbf{z}_{l,m}\|_2^2 + \alpha \|\mathbf{z}_{l,m}\|_0 \right)$$

- ▶ Joint unsupervised clustering / sparsification
- ▶ Further nonconvexity due to clustering
- ▶ Efficient alternating minimization algorithm [126]

Example: 3D X-ray CT learned set of transforms

J. Fessler
Recon

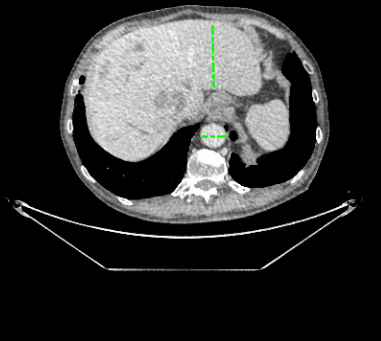


Example: 3D X-ray CT ULTRA for chest scan

J. Fessler
Recon



FDK



PWLS-EP



PWLS-ULTRA



Zheng et al., IEEE T-MI, June 2018 [124] (Special issue on machine learning for image reconstruction)

Matlab code: <http://web.eecs.umich.edu/~fessler/irt/reproduce/>

<https://github.com/xuehangzheng/PWLS-ULTRA-for-Low-Dose-3D-CT-Image-Reconstruction>

Introduction

Brief review of classic methods (> 10 years old)

Sparsity regularizers: Basic

Sparsity regularizers: Advanced

Adaptive regularizers

Population adaptive regularization

Patient adaptive regularization

Example: learned dictionary

Denoising-based “regularization”

Deep-learning approaches for image reconstruction

Looking forward

Bibliography

- ▶ Data
 - ▶ Population adaptive methods
 - ▶ Patient adaptive methods
- ▶ Spatial structure
 - ▶ Patch-based models
 - ▶ Convolutional models
- ▶ Regularizer formulation
 - ▶ Synthesis (dictionary) approach
 - ▶ Analysis (sparsifying transform) approach

Dictionary-blind MR image reconstruction:

$$\hat{\mathbf{x}} = \arg \min_{\mathbf{x}} \frac{1}{2} \|\mathbf{Ax} - \mathbf{y}\|_2^2 + \beta R(\mathbf{x})$$

$$R(\mathbf{x}) = \min_{\mathbf{D} \in \mathcal{D}} \min_{\mathbf{Z}} \sum_{m=1}^M \left(\|\mathbf{P}_m \mathbf{x} - \mathbf{Dz}_m\|_2^2 + \lambda^2 \|\mathbf{z}_m\|_0 \right)$$

where \mathbf{P}_m extracts m th of M image patches.

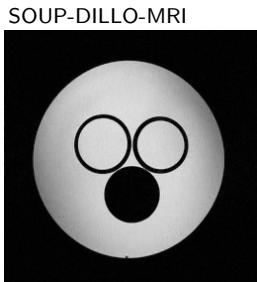
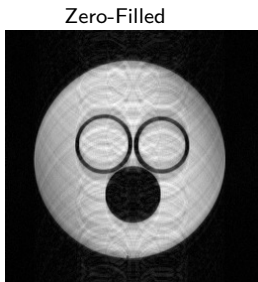
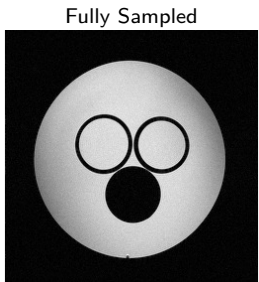
In words: of the many images...

Alternating (nested) minimization:

- ▶ Fixing \mathbf{x} and \mathbf{D} , update each row of $\mathbf{Z} = [\mathbf{z}_1 \dots \mathbf{z}_M]$ sequentially via hard-thresholding.
- ▶ Fixing \mathbf{x} and \mathbf{Z} , update \mathbf{D} using SOUP-DIL [127].
- ▶ Fixing \mathbf{Z} and \mathbf{D} , updating \mathbf{x} is a quadratic problem.
 - Efficient FFT solution for single-coil Cartesian MRI.
 - Use CG for non-Cartesian and/or parallel MRI.
- ▶ Non-convex due to \mathcal{D} , \mathbf{Dz}_m , 0-norm, but monotone decreasing and some convergence theory [127].

2D CS MRI results I

J. Fessler
Recon

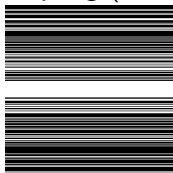


6×6 patches

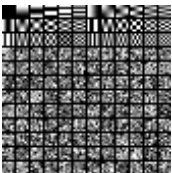
$$\boldsymbol{D} \in \mathbb{C}^{6^2 \times 144}$$

\boldsymbol{D}_0 : [DCT | random]
[127]

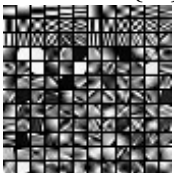
Sampling ($2.5 \times$)



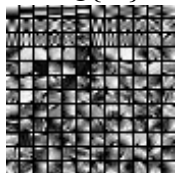
Initial \boldsymbol{D}

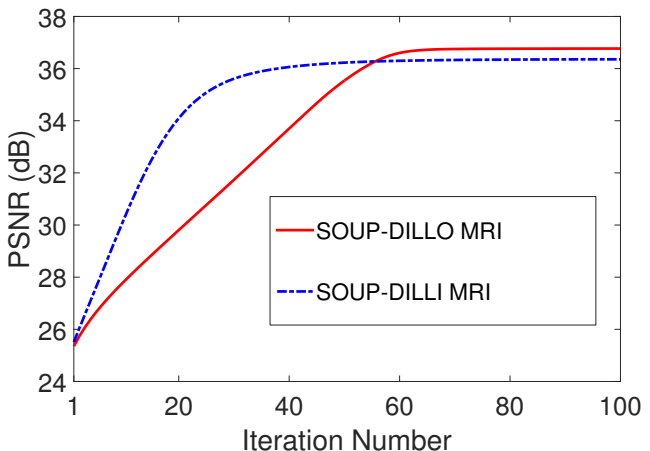


Learned real{ \boldsymbol{D} }



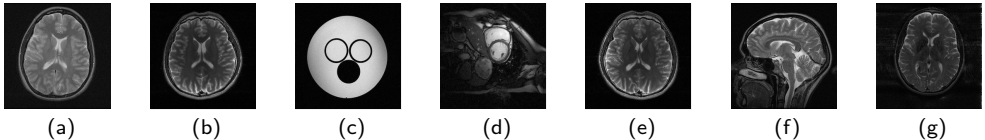
imag{ \boldsymbol{D} }





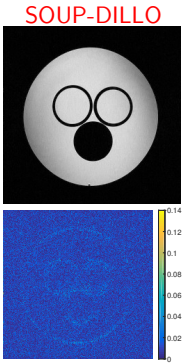
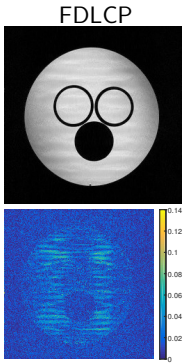
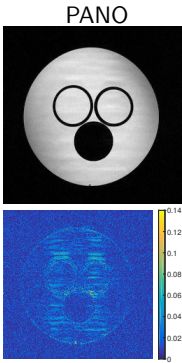
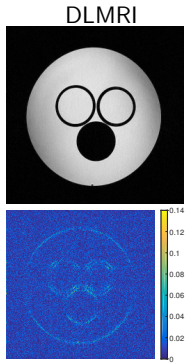
(SNR vs fully sampled image.)
Using $\|z_m\|_0$ leads to higher SNR than $\|z_m\|_1$.
Adaptive case is non-convex anyway...

Matlab code: <http://web.eecs.umich.edu/~fessler/irt/reproduce/>
https://gitlab.eecs.umich.edu/fessler/soupdil_dinokat



PSNR:

Im.	Samp.	Acc.	0-fill	Sparse MRI	PANO	DLMRI	SOUP-DILLI	SOUP-DILLO
a	Cart.	7x	27.9	28.6	31.1	31.1	30.8	31.1
b	Cart.	2.5x	27.7	31.6	41.3	40.2	38.5	42.3
c	Cart.	2.5x	24.9	29.9	34.8	36.7	36.6	37.3
c	Cart.	4x	25.9	28.8	32.3	32.1	32.2	32.3
d	Cart.	2.5x	29.5	32.1	36.9	38.1	36.7	38.4
e	Cart.	2.5x	28.1	31.7	40.0	38.0	37.9	41.5
f	2D rand.	5x	26.3	27.4	30.4	30.5	30.3	30.6
g	Cart.	2.5x	32.8	39.1	41.6	41.7	42.2	43.2
Ref.				[108]	[128]	[114]	[127]	[127]



Summary: 2D static MR reconstruction from under-sampled data with adaptive dictionary learning and convergent algorithm, faster than K-SVD approach of DLMRI.

Introduction

Brief review of classic methods (> 10 years old)

Sparsity regularizers: Basic

Sparsity regularizers: Advanced

Adaptive regularizers

Denoising-based “regularization”

Deep-learning approaches for image reconstruction

Looking forward

Bibliography

Patch-based and convolutional sparsity models lead to a denoising step for the current image estimate x_t at iteration t

Many alternative denoising methods:

- ▶ nonlocal means (NLM) [130]
- ▶ block-matching 3D (BM3D) [131]
- ▶ ...

To adapt most such denoising methods for image reconstruction:

- ▶ plug-and-play ADMM [132, 133]
- ▶ Regularization by denoising (RED) [134, 135, 136]

Introduction

Brief review of classic methods (> 10 years old)

Sparsity regularizers: Basic

Sparsity regularizers: Advanced

Adaptive regularizers

Denoising-based “regularization”

Deep-learning approaches for image reconstruction

Unrolled loops

Challenges and limitations

Momentum-Net

Looking forward

Bibliography

- ▶ Learn sparsifying transform or dictionary for patches from training data
 - interpretable (?) optimization formulations
 - local prior information only (patch size)
 - perhaps slower computation due to optimization iterations
- ▶ Train neural network (aka **deep learning**)
 - less interpretable
 - possibly more global prior information
 - slow training, but perhaps faster computation after trained

Overview:

- ▶ image-domain learning [137, 138]
- ▶ k-space or data-domain learning
 - e.g., RAKI [139], [140]
- ▶ transform learning (direct from k-space to image)
 - e.g., AUTOMAP [141]
- ▶ hybrid-domain learning (unrolled loop, e.g., variational network)
 - alternate between denoising/dealiasing and reconstruction from k-space
 - e.g., [142, 143, 144, 145, 146, 140] ...

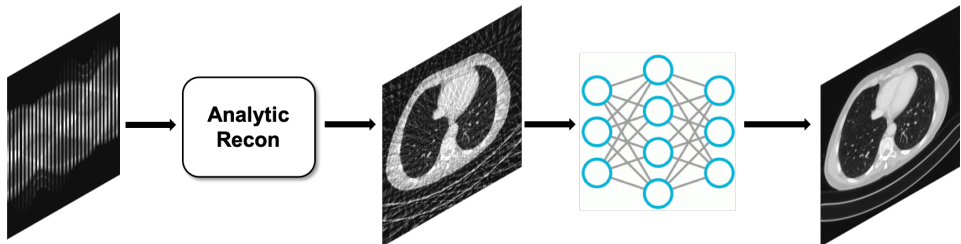


Figure courtesy of Jong Chul Ye, KAIST University.

- + simple and fast
- aliasing is spatially widespread, requires deep network

Investigating Robustness to Unseen Pathologies in Model-Free Deep Multicoil Reconstruction

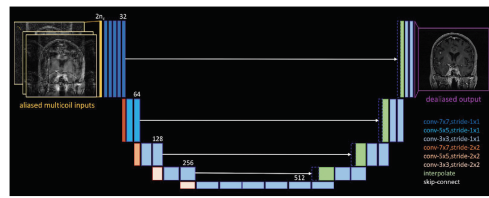
Gopal Nataraj¹ and Ricardo Otazo^{1,2}

¹Dept. of Medical Physics, Memorial Sloan Kettering Cancer Center

²Dept. of Radiology, Memorial Sloan Kettering Cancer Center

Introduction

Speed is often claimed as a key advantage of deep learning (DL) for undersampled parallel MRI reconstruction [1]. However, the only DL approach that to our knowledge has studied generalizability to pathologies unseen in training [2] requires repeated application of the MR acquisition model and its adjoint, just as in iterative methods. In contrast, model-free DL reconstruction has the potential to be much faster. Prior model-free DL work [3] proposes to learn a mapping directly from k-space but with



[147] ISMRM 2020 Workshop on Data Sampling & Image Reconstruction

Dangers of image-domain learning II

J. Fessler
Recon

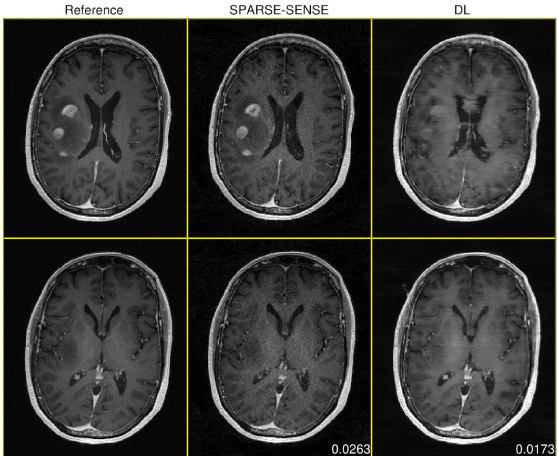


Figure 3: Reconstructions in a case of anaplastic astrocytoma, a rare malignant brain tumor. SPARSE-SENSE and DL reconstructions are from the same 4x-accelerated retrospectively undersampled acquisition. DL achieves lower whole-volume MAE than SPARSE-SENSE, but fails to properly reconstruct regions near the tumor.

- ▶ Use NN output as a “prior” for iterative reconstruction [137, 148]:

$$\hat{\mathbf{x}}_\beta = \arg \min_{\mathbf{x}} \|\mathbf{Ax} - \mathbf{y}\|_2^2 + \beta \|\mathbf{x} - \mathbf{x}_{\text{NN}}\|_2^2 = (\mathbf{A}'\mathbf{A} + \beta \mathbf{I})^{-1}(\mathbf{A}'\mathbf{y} + \beta \mathbf{x}_{\text{NN}})$$

- ▶ For single-coil Cartesian case:
 - no iterations are needed (solve with FFTs)
 - $\lim_{\beta \rightarrow 0} \hat{\mathbf{x}}_\beta$ replaces missing k-space data with FFT of \mathbf{x}_{NN}
- ▶ Iterations needed for parallel MRI and/or non-Cartesian sampling (PCG)

- ▶ Learn residual (aliasing artifacts), then subtract [149, 150]

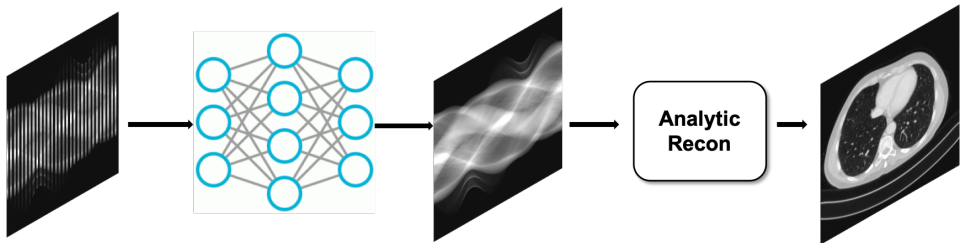


Figure courtesy of Jong Chul Ye, KAIST University.

- + simple and fast (“nonlinear GRAPPA”)
- + “database-free” : learn from auto-calibration data
- perhaps harder to represent local image features?

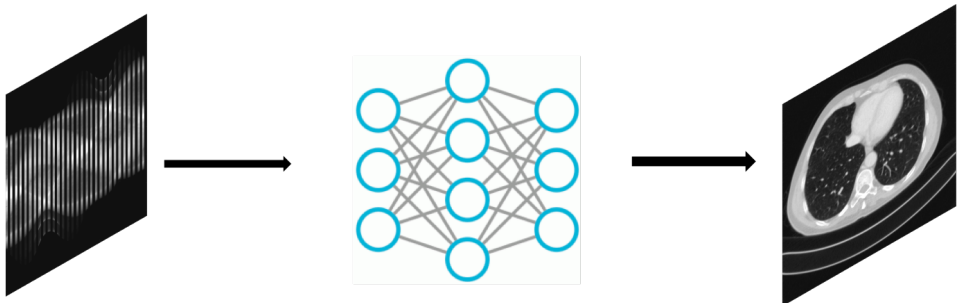


Figure courtesy of Jong Chul Ye, KAIST University.

- + in principle, purely data driven; potential to avoid model mismatch
- high memory requirement for fully connected layers

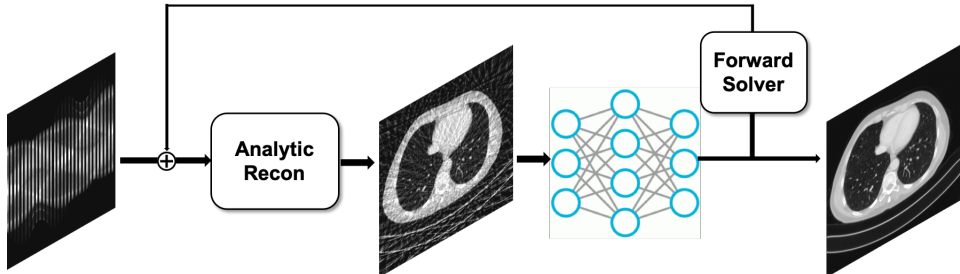


Figure courtesy of Jong Chul Ye, KAIST University.

- + physics-based use of k-space data & image-domain priors
- + interpretable connections to optimization approaches
- more computation due to “iterations” (layers) and repeated FFT/NUFFT

- ▶ learned ISTA (LISTA) [151]
aka proximal gradient method / forward-backward splitting [152]
 - ▶ half-quadratic [153]
 - ▶ reaction-diffusion (GD) [154, 155]
 - ▶ gradient descent / Landweber [156, 143]
 - ▶ ADMM [142, 157]
 - ▶ iterative hard thresholding (IHT) [158]
 - ▶ approximate message passing (AMP) [159]
 - ▶ accelerated gradient method [160]
 - ▶ primal dual [161]
 - ▶ primal dual with line search [162]
 - ▶ alternating minimization [163]
 - ▶ block coordinate descent (BCD-Net) [164, 165, 166]
 - ▶ block proximal gradient with momentum (BPGM: Momentum-Net) [167, 3]
 - ▶ And more [168, 62, 169, 170, 171, 172]
- Surveys: [173, 174]

- ML-based nonlinear encoder, e.g., autoencoder or generative adversarial network (GAN) [175, 176]: nonlinear generalizations of subspace models
- learn G : maps low-dimensional latent parameter \mathbf{z} into high-dimensional image \mathbf{x}
 - ▶ Synthesis form [177]:

$$\hat{\mathbf{x}} = G(\hat{\mathbf{z}}), \quad \hat{\mathbf{z}} = \arg \min_{\mathbf{z}} \|\mathbf{A}G(\mathbf{z}) - \mathbf{y}\|_2^2$$

Caveat: $\hat{\mathbf{x}} \in \text{Range}(G)$, non-convex minimization

- ML-based nonlinear encoder, e.g., autoencoder or generative adversarial network (GAN) [175, 176]: nonlinear generalizations of subspace models
- learn G : maps low-dimensional latent parameter \mathbf{z} into high-dimensional image \mathbf{x}
 - ▶ Synthesis form [177]:

$$\hat{\mathbf{x}} = G(\hat{\mathbf{z}}), \quad \hat{\mathbf{z}} = \arg \min_{\mathbf{z}} \|\mathbf{A}G(\mathbf{z}) - \mathbf{y}\|_2^2$$

Caveat: $\hat{\mathbf{x}} \in \text{Range}(G)$, non-convex minimization

- ▶ Regularizer form:

$$\hat{\mathbf{x}} = \arg \min_{\mathbf{x}} \|\mathbf{A}\mathbf{x} - \mathbf{y}\|_2^2 + \beta R_{\text{encoder}}(\mathbf{x})$$

$$R_{\text{encoder}}(\mathbf{x}) = \min_{\mathbf{z}} \|\mathbf{x} - G(\mathbf{z})\|_p^p$$

Caveat: expensive non-convex double minimization, but more robust to encoder

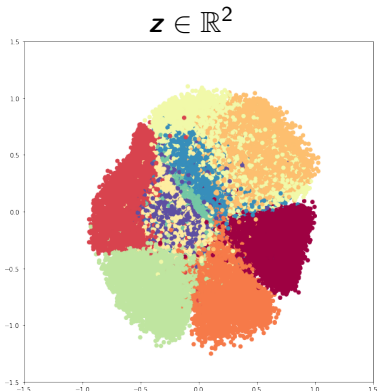
Nonlinear encoder illustration

J. Fessler
Recon

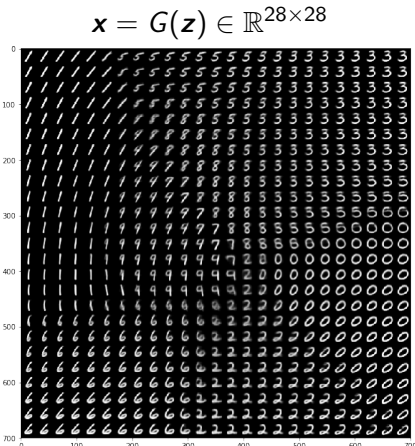


From jupyter notebook for [178] (13 layer CNN with $\approx 300K$ learned parameters) at

https://github.com/skolouri/swae/blob/master/MNIST_SlicedWassersteinAutoEncoder_Circle.ipynb



\mapsto



Caveat: Where is 4?

Generative Adversarial Networks (GAN) example

J. Fessler
Recon



From Google's [179]:



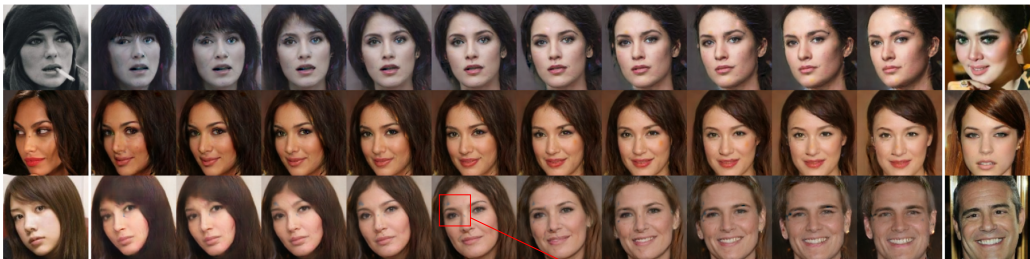
Much more realistic than linear interpolation (averaging)
“setting a new milestone in visual quality” [179]

Generative Adversarial Networks (GAN) example

J. Fessler
Recon



From Google's [179]:



Caveat: non-physical output



Model based image reconstruction using deep learned priors (MODL) [169, 62]

$$\hat{\mathbf{x}} = \arg \min_{\mathbf{x}} \frac{1}{2} \|\mathbf{A}\mathbf{x} - \mathbf{y}\|_2^2 + \|\text{CNN}(\mathbf{x})\|_2^2$$

- ▶ $\text{CNN}(\mathbf{x}) = \mathbf{x} - \text{denoise}(\mathbf{x})$ predicts noise and aliasing patterns
(*cf.* ResNet principle [149])
- ▶ Demonstrated robustness to changes in acceleration factors

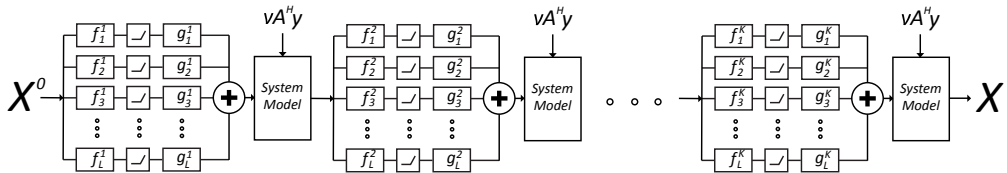
- ▶ Training data size (but self supervision [180])
- ▶ Local minimizers of training loss functions
- ▶ Sensitivity to adversarial examples (for classification problems)
- ▶ Enormous design space (architectures, parameters)
- ▶ Training loss functions, evaluation metrics vs clinical tasks
- ▶ Generalizability
 - noise level
 - coil sensitivity
 - k-space sampling
- ▶ Stability [181]
- ▶ Memory (especially 3D and dynamic)
- ▶ ...

Caveat: careful comparisons needed I

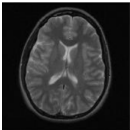
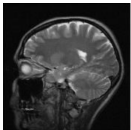
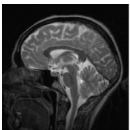
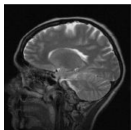
J. Fessler
Recon



Unrolled loop method with 20 layers trained with $1.3 \cdot 10^6$ MR image 8×8 patches
[163]



Tested with 5 different images:



Caveat: careful comparisons needed II

J. Fessler
Recon



Results:

UF	Image	Zero-filled	Sparse MRI	UTMRI	Proposed
3.3×	1	25.6	26.7	28.3	28.2
	2	25.2	26.6	27.9	27.8
	3	26.0	27.3	29.3	28.9
	4	25.4	26.7	28.2	28.1
	5	27.2	28.9	30.6	30.3
Avg. PSNR change	-	-	1.36	2.98	2.78
5×	1	24.7	25.9	27.6	27.5
	2	24.2	25.5	27.2	27.0
	3	24.9	26.3	28.5	28.0
	4	24.4	25.7	27.6	27.4
	5	26.2	27.9	29.8	29.5
Avg. PSNR change	-	-	1.38	3.26	3.0
Approx recon time	-	-	100s	240s	50s

Sparse MRI [35] total variation and wavelets

UTMRI [126] (union of learned sparsifying transforms): adaptive, not “deep”

Introduction

Brief review of classic methods (> 10 years old)

Sparsity regularizers: Basic

Sparsity regularizers: Advanced

Adaptive regularizers

Denoising-based “regularization”

Deep-learning approaches for image reconstruction

Unrolled loops

Challenges and limitations

Momentum-Net

Looking forward

Bibliography

Cost function for convolutional sparsity regularization:

$$\arg \min_{\mathbf{x}} \frac{1}{2} \|\mathbf{A}\mathbf{x} - \mathbf{y}\|_{\mathbf{W}}^2 + \beta \left(\min_{\zeta} \sum_{k=1}^K \frac{1}{2} \|\mathbf{h}_k * \mathbf{x} - \zeta_k\|_2^2 + \alpha \|\zeta_k\|_1 \right)$$

Alternating minimization updates:

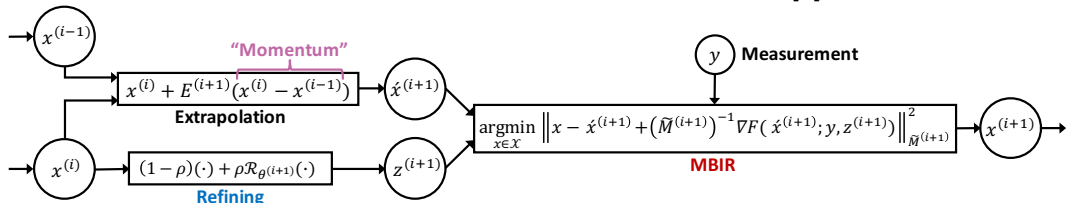
Sparse code: $\zeta_k^{(i+1)} = \text{soft}\left\{\mathbf{h}_k * \mathbf{x}^{(i)}, \alpha\right\}$

Image: $\mathbf{x}^{(i+1)} = \arg \min_{\mathbf{x}} F(\mathbf{x}; \mathbf{y}, \mathbf{z}^{(i)})$

$$\begin{aligned} F(\mathbf{x}; \mathbf{y}, \mathbf{z}^{(i)}) &\triangleq \frac{1}{2} \|\mathbf{A}\mathbf{x} - \mathbf{y}\|_{\mathbf{W}}^2 + \beta \left(\sum_{k=1}^K \frac{1}{2} \left\| \mathbf{h}_k * \mathbf{x} - \zeta_k^{(i+1)} \right\|_2^2 + \alpha \left\| \zeta_k^{(i+1)} \right\|_1 \right) \\ &= \frac{1}{2} \|\mathbf{A}\mathbf{x} - \mathbf{y}\|_{\mathbf{W}}^2 + \beta \frac{1}{2} \left\| \mathbf{x} - \mathbf{z}^{(i)} \right\|_2^2 \quad (\text{quadratic but } \text{large} \implies \text{majorize}) \end{aligned}$$

$$\mathbf{z}^{(i)} = \mathcal{R}(\mathbf{z}^{(i)}) = \sum_{k=1}^K \text{flip}(\mathbf{h}_k) * \text{soft}\left\{\mathbf{h}_k * \mathbf{x}^{(i)}\right\} \quad (\text{denoise} \implies \text{learn})$$

Unrolled loop network with momentum and quadratic majorizer [3]:



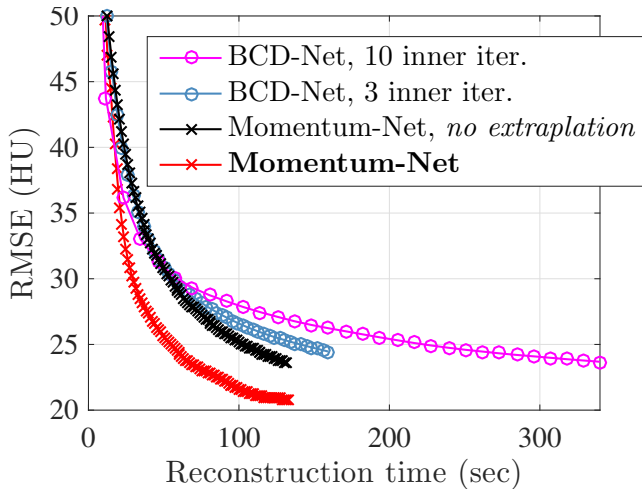
- ▶ Diagonal majorizer for CT: $\mathbf{M} = \text{Diag}\{\mathbf{A}' \mathbf{W} \mathbf{A} \mathbf{1}\} + \beta \mathbf{I} \succeq \mathbf{A}' \mathbf{W} \mathbf{A} + \beta \mathbf{I}$
- ▶ Learn image mapper (“refiner”) \mathcal{R} from training data (supervised).
cf CNN: filter → threshold → filter

- ▶ Image mapper \mathcal{R} is **shallow**
 \implies less risk of over-fitting / hallucination
- ▶ Momentum accelerates convergence \implies fewer “layers” (outer iterations)
- ▶ First unrolled loop approach to have convergence theory
(under suitable assumptions on \mathcal{R})
- ▶ Image update uses original measurements \mathbf{y} and imaging physics \mathbf{A}

[3] Il Yong Chun, Zhengyu Huang, Hongki Lim, J A Fessler
Momentum-Net: Fast and convergent iterative neural network for inverse problems

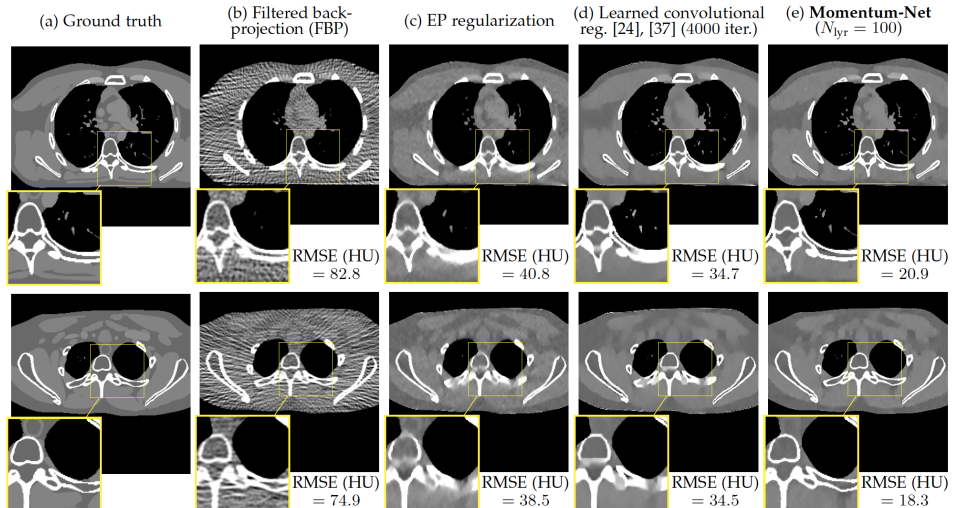
<http://arxiv.org/abs/1907.11818>

Illustration of benefits of momentum:



Momentum-Net preliminary image results

J. Fessler
Recon



Sparse-view CT with 123/984 views, $I_0 = 10^5$, 800-1200 mod. HU display.

Introduction

Brief review of classic methods (> 10 years old)

Sparsity regularizers: Basic

Sparsity regularizers: Advanced

Adaptive regularizers

Denoising-based “regularization”

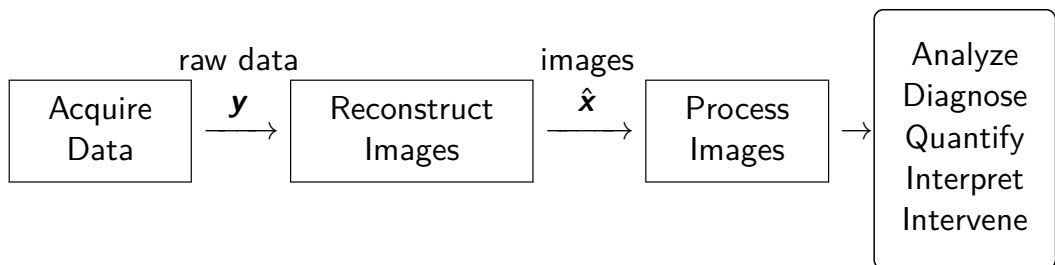
Deep-learning approaches for image reconstruction

Looking forward

Bibliography

- ▶ All presented sparsity models are applicable
- ▶ and many more: low rank, tensors...
- ▶ Challenge for supervised ML methods: all dynamic scans are under-sampled
- ▶ DL methods are appearing, e.g., [144]

Overview of medical imaging:

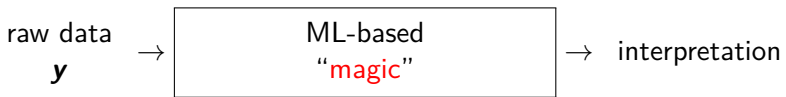


A more speculative opportunity for machine learning:



...

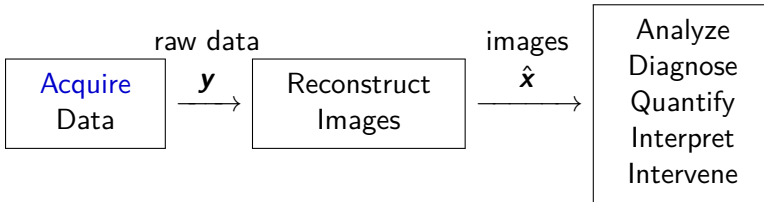
A more speculative opportunity for machine learning:



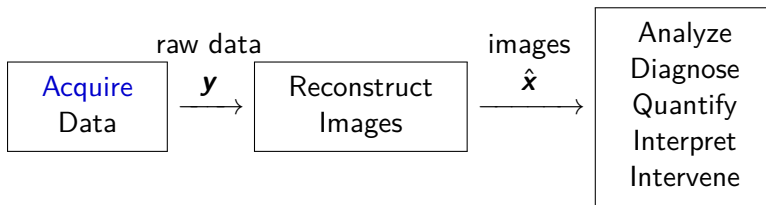
- ▶ CT sinogram to vessel diameter [182, 183]
- ▶ k-space to ???

Caveat: seeing is believing...

One more opportunity for ML in medical imaging:



One more opportunity for ML in medical imaging:



k-space sampling design using ML methods:

“Learning-based compressive MRI” [25, 184]

(Volkan Cevher group, June 2018 IEEE T-MI)

Caveat: single coil only so far; hard to generalize to parallel MRI?

Thanks to numerous graduate students, postdocs, collaborators.

Especially for the results shown in this talk:

Prof. Sai Ravishankar, Prof. Il Yong Chun, Prof. Donghwan Kim, Prof. Yong Long,
Xuehang Zheng,
Prof. Raj Nadakuditi, Prof. Doug Noll

Talk: <http://web.eecs.umich.edu/~fessler/papers/files/talk/20/siam.pdf>
code: <https://github.com/JeffFessler/MIRT.jl>



- [1] S. Ravishankar, J. C. Ye, and J. A. Fessler. "Image reconstruction: from sparsity to data-adaptive methods and machine learning." In: *Proc. IEEE* 108.1 (Jan. 2020), 86–109. DOI: [10.1109/JPROC.2019.2936204](https://doi.org/10.1109/JPROC.2019.2936204) (cit. on p. 2).
- [2] J. A. Fessler. "Optimization methods for MR image reconstruction." In: *IEEE Sig. Proc. Mag.* 37.1 (Jan. 2020), 33–40. DOI: [10.1109/MSP.2019.2943645](https://doi.org/10.1109/MSP.2019.2943645) (cit. on p. 2).
- [3] I. Y. Chun et al. *Momentum-Net: Fast and convergent iterative neural network for inverse problems*. 2019. URL: <http://arxiv.org/abs/1907.11818> (cit. on pp. 2, 85, 97, 98).
- [4] M. K. Stehling, R. Turner, and P. Mansfield. "Echo-planar imaging: magnetic resonance imaging in a fraction of a second." In: *Science* 254.5028 (Oct. 1991), 43–50. DOI: [10.1126/science.1925560](https://doi.org/10.1126/science.1925560) (cit. on p. 5).
- [5] P. Mansfield, R. Coxon, and J. Hykin. "Echo-volumar imaging (EVI) of the brain at 3.0 T: first normal volunteer and functional imaging results." In: *J. Comp. Assisted Tomo.* 19.6 (Nov. 1995), 847–52 (cit. on p. 5).
- [6] A. Macovski. "Volumetric NMR imaging with time-varying gradients." In: *Mag. Res. Med.* 2.1 (Feb. 1985), 29–40. DOI: [10.1002/mrm.1910020105](https://doi.org/10.1002/mrm.1910020105) (cit. on p. 5).
- [7] C. H. Meyer et al. "Fast spiral coronary artery imaging." In: *Mag. Res. Med.* 28.2 (Dec. 1992), 202–13. DOI: [10.1002/mrm.1910280204](https://doi.org/10.1002/mrm.1910280204) (cit. on p. 5).
- [8] D. A. Feinberg et al. "Halving MR imaging time by conjugation: demonstration at 3.5 kG." In: *Radiology* 161.2 (Nov. 1986), 527–31. DOI: [10.1148/radiology.161.2.3763926](https://doi.org/10.1148/radiology.161.2.3763926) (cit. on p. 5).
- [9] P. Margosian, F. Schmitt, and D. E. Purdy. "Faster MR imaging: Imaging with half the data." In: *Health Care Instrum.* 1.6 (1986), 195–7 (cit. on p. 5).
- [10] D. C. Noll, D. G. Nishimura, and A. Macovski. "Homodyne detection in magnetic resonance imaging." In: *IEEE Trans. Med. Imag.* 10.2 (June 1991), 154–63. DOI: [10.1109/42.79473](https://doi.org/10.1109/42.79473) (cit. on p. 5).
- [11] J. W. Carlson. "An algorithm for NMR imaging reconstruction based on multiple RF receiver coils." In: *J. Mag. Res.* 74.2 (Sept. 1987), 376–80. DOI: [10.1016/0022-2364\(87\)90348-9](https://doi.org/10.1016/0022-2364(87)90348-9) (cit. on p. 5).

- [12] M. Hutchinson and U. Raff. "Fast MRI data acquisition using multiple detectors." In: *Mag. Res. Med.* 6.1 (Jan. 1988), 87–91. doi: [10.1002/mrm.1910060110](https://doi.org/10.1002/mrm.1910060110) (cit. on p. 5).
- [13] P. B. Roemer et al. "The NMR phased array." In: *Mag. Res. Med.* 16.2 (Nov. 1990), 192–225. doi: [10.1002/mrm.1910160203](https://doi.org/10.1002/mrm.1910160203) (cit. on pp. 5, 13).
- [14] J. B. Ra and C. Y. Rim. "Fast imaging using subencoding data sets from multiple detectors." In: *Mag. Res. Med.* 30.1 (July 1993), 142–5. doi: [10.1002/mrm.1910300123](https://doi.org/10.1002/mrm.1910300123) (cit. on p. 5).
- [15] D. K. Sodickson and W. J. Manning. "Simultaneous acquisition of spatial harmonics (SMASH): Fast imaging with radiofrequency coil arrays." In: *Mag. Res. Med.* 38.4 (Oct. 1997), 591–603. doi: [10.1002/mrm.1910380414](https://doi.org/10.1002/mrm.1910380414) (cit. on p. 5).
- [16] K. P. Pruessmann et al. "SENSE: sensitivity encoding for fast MRI." In: *Mag. Res. Med.* 42.5 (Nov. 1999), 952–62. doi: [10.1002/\(SICI\)1522-2594\(199911\)42:5<952::AID-MRM16>3.0.CO;2-S](https://doi.org/10.1002/(SICI)1522-2594(199911)42:5<952::AID-MRM16>3.0.CO;2-S) (cit. on pp. 5, 10, 13).
- [17] K. P. Pruessmann et al. "Advances in sensitivity encoding with arbitrary k-space trajectories." In: *Mag. Res. Med.* 46.4 (Oct. 2001), 638–51. doi: [10.1002/mrm.1241](https://doi.org/10.1002/mrm.1241) (cit. on pp. 5, 14).
- [18] M. A. Griswold et al. "Generalized autocalibrating partially parallel acquisitions (GRAPPA)." In: *Mag. Res. Med.* 47.6 (June 2002), 1202–10. doi: [10.1002/mrm.10171](https://doi.org/10.1002/mrm.10171) (cit. on pp. 5, 37).
- [19] Y. Cao and D. N. Levin. "Feature-recognizing MRI." In: *Mag. Res. Med.* 30.3 (Sept. 1993), 305–17. doi: [10.1002/mrm.1910300306](https://doi.org/10.1002/mrm.1910300306) (cit. on p. 5).
- [20] N. Chauffert et al. "Variable density sampling with continuous trajectories." In: *SIAM J. Imaging Sci.* 7.4 (2014), 1962–92. doi: [10.1137/130946642](https://doi.org/10.1137/130946642) (cit. on p. 5).
- [21] C. Boyer et al. "On the generation of sampling schemes for magnetic resonance imaging." In: *SIAM J. Imaging Sci.* 9.4 (2016), 2039–72. doi: [10.1137/16m1059205](https://doi.org/10.1137/16m1059205) (cit. on p. 5).

- [22] N. Chauffert et al. "A projection algorithm for gradient waveforms design in magnetic resonance imaging." In: *IEEE Trans. Med. Imag.* 35.9 (Sept. 2016), 2026–39. DOI: [10.1109/tmi.2016.2544251](https://doi.org/10.1109/tmi.2016.2544251) (cit. on p. 5).
- [23] C. Lazarus et al. "SPARKLING: variable-density k-space filling curves for accelerated T2*-weighted MRI." In: *Mag. Res. Med.* 81.6 (June 2019), 3643–61. DOI: [10.1002/mrm.27678](https://doi.org/10.1002/mrm.27678) (cit. on p. 5).
- [24] S. Ravishankar and Y. Bresler. "Adaptive sampling design for compressed sensing MRI." In: *Proc. Int'l. Conf. IEEE Engr. in Med. and Biol. Soc.* 2011, 3751–5. DOI: [10.1109/IEMBS.2011.6090639](https://doi.org/10.1109/IEMBS.2011.6090639) (cit. on p. 5).
- [25] L. Baldassarre et al. "Learning-based compressive subsampling." In: *IEEE J. Sel. Top. Sig. Proc.* 10.4 (June 2016), 809–22. DOI: [10.1109/jstsp.2016.2548442](https://doi.org/10.1109/jstsp.2016.2548442) (cit. on pp. 5, 107).
- [26] G. Godaliyadda et al. "A framework for dynamic image sampling based on supervised learning." In: *IEEE Trans. Computational Imaging* 4.1 (Mar. 2018), 1–16. DOI: [10.1109/tci.2017.2777482](https://doi.org/10.1109/tci.2017.2777482) (cit. on p. 5).
- [27] C. D. Bahadir, A. V. Dalca, and M. R. Sabuncu. "Learning-based optimization of the under-sampling pattern in MRI." In: *Information Processing in Medical Im.* 2019, 780–92. DOI: [10.1007/978-3-030-20351-1_61](https://doi.org/10.1007/978-3-030-20351-1_61) (cit. on p. 5).
- [28] H. K. Aggarwal and M. Jacob. "Joint optimization of sampling pattern and priors in model based deep learning." In: *Proc. IEEE Intl. Symp. Biomed. Imag.* 2020, 926–9. DOI: [10.1109/ISBI45749.2020.9098639](https://doi.org/10.1109/ISBI45749.2020.9098639) (cit. on p. 5).
- [29] E. Candes et al. "Image reconstruction from highly undersampled data using total variation minimization." In: *MRA Workshop, Oct. 8, London Ontario.* 2004, p. 147 (cit. on p. 5).
- [30] M. Lustig et al. "Faster imaging with randomly perturbed, undersampled spirals and $|L|_1$ reconstruction." In: *Proc. Int'l. Soc. Mag. Res. Med.* 2005, p. 685. URL: <http://cds.ismrm.org/ismrm-2005/Files/00685.pdf> (cit. on p. 5).
- [31] S. J. LaRoque, E. Y. Sidky, and X. Pan. "Image Reconstruction from Sparse Data in Echo-Planar Imaging." In: *Proc. IEEE Nuc. Sci. Symp. Med. Im. Conf.* Vol. 5. 2006, 3166–9. DOI: [10.1109/NSSMIC.2006.356547](https://doi.org/10.1109/NSSMIC.2006.356547) (cit. on p. 5).

- [32] M. Lustig, D. L. Donoho, and J. M. Pauly. "Rapid MR imaging with "compressed sensing" and randomly under-sampled 3DFT trajectories." In: *Proc. Intl. Soc. Mag. Res. Med.* 2006, p. 695. URL: <http://dev.ismrm.org//2006/0695.html> (cit. on p. 5).
- [33] K. T. Block, M. Uecker, and J. Frahm. "Undersampled radial MRI with multiple coils. Iterative image reconstruction using a total variation constraint." In: *Mag. Res. Med.* 57.6 (June 2007), 1086–98. DOI: [10.1002/mrm.21236](https://doi.org/10.1002/mrm.21236) (cit. on pp. 5, 27).
- [34] E. Candes and J. Romberg. "Sparsity and incoherence in compressive sampling." In: *Inverse Prob.* 23.3 (June 2007), 969–86. DOI: [10.1088/0266-5611/23/3/008](https://doi.org/10.1088/0266-5611/23/3/008) (cit. on p. 5).
- [35] M. Lustig, D. Donoho, and J. M. Pauly. "Sparse MRI: The application of compressed sensing for rapid MR imaging." In: *Mag. Res. Med.* 58.6 (Dec. 2007), 1182–95. DOI: [10.1002/mrm.21391](https://doi.org/10.1002/mrm.21391) (cit. on pp. 5, 10, 94).
- [36] J. C. Ye et al. "Projection reconstruction MR imaging using FOCUSS." In: *Mag. Res. Med.* 57.4 (Apr. 2007), 764–75. DOI: [10.1002/mrm.21202](https://doi.org/10.1002/mrm.21202) (cit. on pp. 5, 29).
- [37] E. J. Candes and M. B. Wakin. "An introduction to compressive sampling." In: *IEEE Sig. Proc. Mag.* 25.2 (Mar. 2008), 21–30. DOI: [10.1109/MSP.2007.914731](https://doi.org/10.1109/MSP.2007.914731) (cit. on p. 5).
- [38] M. Lustig et al. "Compressed sensing MRI." In: *IEEE Sig. Proc. Mag.* 25.2 (Mar. 2008), 72–82. DOI: [10.1109/MSP.2007.914728](https://doi.org/10.1109/MSP.2007.914728) (cit. on pp. 5, 27).
- [39] FDA. *510k premarket notification of HyperSense (GE Medical Systems)*. 2017. URL: <https://www.accessdata.fda.gov/scripts/cdrh/cfdocs/cfpmn/pmn.cfm?ID=K162722> (cit. on p. 5).
- [40] FDA. *510k premarket notification of Compressed Sensing Cardiac Cine (Siemens)*. 2017. URL: <https://www.accessdata.fda.gov/scripts/cdrh/cfdocs/cfpmn/pmn.cfm?ID=K163312> (cit. on p. 5).
- [41] FDA. *510k premarket notification of Compressed SENSE*. 2018. URL: https://www.accessdata.fda.gov/cdrh_docs/pdf17/K173079.pdf (cit. on p. 5).

- [42] L. Geerts-Ossevoort et al. *Compressed SENSE*. Philips white paper 4522 991 31821 Nov. 2018. 2018. URL: <https://philipsproductcontent.blob.core.windows.net/assets/20180109/619119731f2a42c4acd4a863008a46c7.pdf> (cit. on p. 5).
- [43] G. Harikumar, C. Couvreur, and Y. Bresler. "Fast optimal and suboptimal algorithms for sparse solutions to linear inverse problems." In: *Proc. IEEE Conf. Acoust. Speech Sig. Proc.* Vol. 3. 1998, 1877–80. DOI: [10.1109/ICASSP.1998.681830](https://doi.org/10.1109/ICASSP.1998.681830) (cit. on p. 5).
- [44] J. Hamilton, D. Franson, and N. Seiberlich. "Recent advances in parallel imaging for MRI." In: *Prog. in Nuclear Magnetic Resonance Spectroscopy* 101 (Aug. 2017), 71–95. DOI: [10.1016/j.pnmrs.2017.04.002](https://doi.org/10.1016/j.pnmrs.2017.04.002).
- [45] P. J. Shin et al. "Calibrationless parallel imaging reconstruction based on structured low-rank matrix completion." In: *Mag. Res. Med.* 72.4 (Oct. 2014), 959–70. DOI: [10.1002/mrm.24997](https://doi.org/10.1002/mrm.24997) (cit. on pp. 6, 38).
- [46] A. Balachandrasekaran, M. Mani, and M. Jacob. *Calibration-free B0 correction of EPI data using structured low rank matrix recovery*. 2018. URL: <http://arxiv.org/abs/1804.07436> (cit. on pp. 6, 38).
- [47] J. P. Haldar and K. Setsompop. "Linear predictability in MRI reconstruction: Leveraging shift-invariant Fourier structure for faster and better imaging." In: *IEEE Sig. Proc. Mag.* 37.1 (Jan. 2020), 69–82. DOI: [10.1109/MSP.2019.2949570](https://doi.org/10.1109/MSP.2019.2949570) (cit. on p. 6).
- [48] H-L. M. Cheng et al. "Practical medical applications of quantitative MR relaxometry." In: *J. Mag. Res. Im.* 36.4 (Oct. 2012), 805–24. DOI: [10.1002/jmri.23718](https://doi.org/10.1002/jmri.23718) (cit. on p. 6).
- [49] B. Zhao, F. Lam, and Z-P. Liang. "Model-based MR parameter mapping with sparsity constraints: parameter estimation and performance bounds." In: *IEEE Trans. Med. Imag.* 33.9 (Sept. 2014), 1832–44. DOI: [10.1109/TMI.2014.2322815](https://doi.org/10.1109/TMI.2014.2322815) (cit. on p. 6).
- [50] G. Nataraj et al. "Dictionary-free MRI PERK: Parameter estimation via regression with kernels." In: *IEEE Trans. Med. Imag.* 37.9 (Sept. 2018), 2103–14. DOI: [10.1109/TMI.2018.2817547](https://doi.org/10.1109/TMI.2018.2817547) (cit. on p. 6).
- [51] B. B. Mehta et al. "Magnetic resonance fingerprinting: a technical review." In: *Mag. Res. Med.* 81.1 (Jan. 2019), 25–46. DOI: [10.1002/mrm.27403](https://doi.org/10.1002/mrm.27403) (cit. on p. 6).

- [52] J. Bezanson et al. "Julia: A fresh approach to numerical computing." In: *SIAM Review* 59.1 (2017), 65–98. DOI: [10.1137/141000671](https://doi.org/10.1137/141000671) (cit. on p. 7).
- [53] G. A. Wright. "Magnetic resonance imaging." In: *IEEE Sig. Proc. Mag.* 14.1 (Jan. 1997), 56–66. DOI: [10.1109/79.560324](https://doi.org/10.1109/79.560324).
- [54] M. Doneva. "Mathematical models for magnetic resonance imaging reconstruction: an overview of the approaches, problems, and future research areas." In: *IEEE Sig. Proc. Mag.* 37.1 (Jan. 2020), 24–32. DOI: [10.1109/MSP.2019.2936964](https://doi.org/10.1109/MSP.2019.2936964).
- [55] J. A. Fessler. "Model-based image reconstruction for MRI." In: *IEEE Sig. Proc. Mag.* 27.4 (July 2010). Invited submission to special issue on medical imaging, 81–9. DOI: [10.1109/MSP.2010.936726](https://doi.org/10.1109/MSP.2010.936726) (cit. on p. 11).
- [56] J. A. Fessler and B. P. Sutton. "Nonuniform fast Fourier transforms using min-max interpolation." In: *IEEE Trans. Sig. Proc.* 51.2 (Feb. 2003), 560–74. DOI: [10.1109/TSP.2002.807005](https://doi.org/10.1109/TSP.2002.807005) (cit. on p. 10).
- [57] B. P. Sutton, D. C. Noll, and J. A. Fessler. "Fast, iterative image reconstruction for MRI in the presence of field inhomogeneities." In: *IEEE Trans. Med. Imag.* 22.2 (Feb. 2003), 178–88. DOI: [10.1109/TMI.2002.808360](https://doi.org/10.1109/TMI.2002.808360) (cit. on pp. 10, 14).
- [58] A. Macovski. "Noise in MRI." In: *Mag. Res. Med.* 36.3 (Sept. 1996), 494–7. DOI: [10.1002/mrm.1910360327](https://doi.org/10.1002/mrm.1910360327) (cit. on p. 11).
- [59] J. A. Fessler et al. "Toeplitz-based iterative image reconstruction for MRI with correction for magnetic field inhomogeneity." In: *IEEE Trans. Sig. Proc.* 53.9 (Sept. 2005), 3393–402. DOI: [10.1109/TSP.2005.853152](https://doi.org/10.1109/TSP.2005.853152) (cit. on p. 14).
- [60] R. H. Chan and M. K. Ng. "Conjugate gradient methods for Toeplitz systems." In: *SIAM Review* 38.3 (Sept. 1996), 427–82. DOI: [10.1137/S003614494276474](https://doi.org/10.1137/S003614494276474) (cit. on p. 14).
- [61] S. Ramani and J. A. Fessler. "Parallel MR image reconstruction using augmented Lagrangian methods." In: *IEEE Trans. Med. Imag.* 30.3 (Mar. 2011), 694–706. DOI: [10.1109/TMI.2010.2093536](https://doi.org/10.1109/TMI.2010.2093536) (cit. on pp. 14, 30, 33).
- [62] H. K. Aggarwal, M. P. Mani, and M. Jacob. "MoDL: model-based deep learning architecture for inverse problems." In: *IEEE Trans. Med. Imag.* 38.2 (Feb. 2019), 394–405. DOI: [10.1109/tmi.2018.2865356](https://doi.org/10.1109/tmi.2018.2865356) (cit. on pp. 14, 85, 91).

- [63] R. Boubertakh et al. "Non-quadratic convex regularized reconstruction of MR images from spiral acquisitions." In: *Signal Processing* 86.9 (Sept. 2006), 2479–94. DOI: [10.1016/j.sigpro.2005.11.011](https://doi.org/10.1016/j.sigpro.2005.11.011) (cit. on p. 15).
- [64] S. Husse, Y. Goussard, and M. Idiert. "Extended forms of Geman & Yang algorithm: application to MRI reconstruction." In: *Proc. IEEE Conf. Acoust. Speech Sig. Proc.* Vol. 3. 2004, 513–16. DOI: [10.1109/ICASSP.2004.1326594](https://doi.org/10.1109/ICASSP.2004.1326594) (cit. on p. 15).
- [65] A. Florescu et al. "A majorize-minimize memory gradient method for complex-valued inverse problems." In: *Signal Processing* 103 (Oct. 2014), 285–95. DOI: [10.1016/j.sigpro.2013.09.026](https://doi.org/10.1016/j.sigpro.2013.09.026) (cit. on pp. 15, 16).
- [66] S. Geman and D. Geman. "Stochastic relaxation, Gibbs distributions, and Bayesian restoration of images." In: *IEEE Trans. Patt. Anal. Mach. Int.* 6.6 (Nov. 1984), 721–41. DOI: [10.1109/TPAMI.1984.4767596](https://doi.org/10.1109/TPAMI.1984.4767596) (cit. on p. 15).
- [67] J. Besag. "On the statistical analysis of dirty pictures." In: *J. Royal Stat. Soc. Ser. B* 48.3 (1986), 259–302. URL: <http://www.jstor.org/stable/2345426> (cit. on p. 15).
- [68] D. Kim and J. A. Fessler. "Optimized first-order methods for smooth convex minimization." In: *Mathematical Programming* 159.1 (Sept. 2016), 81–107. DOI: [10.1007/s10107-015-0949-3](https://doi.org/10.1007/s10107-015-0949-3) (cit. on p. 16).
- [69] Y. Drori. "The exact information-based complexity of smooth convex minimization." In: *J. Complexity* 39 (Apr. 2017), 1–16. DOI: [10.1016/j.jco.2016.11.001](https://doi.org/10.1016/j.jco.2016.11.001) (cit. on p. 16).
- [70] Y. Nesterov. "A method of solving a convex programming problem with convergence rate $O(1/k^2)$." In: *Soviet Math. Dokl.* 27.2 (1983), 372–76. URL: <http://www.core.ucl.ac.be/~nesterov/Research/Papers/DAN83.pdf> (cit. on p. 16).
- [71] Y. Drori and A. B. Taylor. "Efficient first-order methods for convex minimization: a constructive approach." In: *Mathematical Programming* (2020). DOI: [10.1007/s10107-019-01410-2](https://doi.org/10.1007/s10107-019-01410-2) (cit. on p. 16).
- [72] F. Knoll et al. "Advancing machine learning for MR image reconstruction with an open competition: Overview of the 2019 fastMRI challenge." In: *Mag. Res. Med.* (2020). DOI: [10.1002/mrm.28338](https://doi.org/10.1002/mrm.28338) (cit. on p. 19).

- [73] R. Tibshirani. "Regression shrinkage and selection via the LASSO." In: *J. Royal Stat. Soc. Ser. B* 58.1 (1996), 267–88. URL: <http://www.jstor.org/stable/2346178> (cit. on p. 21).
- [74] E. J. Candes and Y. Plan. "Near-ideal model selection by ℓ_1 minimization." In: *Ann. Stat.* 37.5a (2009), 2145–77. DOI: [10.1214/08-AOS653](https://doi.org/10.1214/08-AOS653) (cit. on p. 21).
- [75] A. B. Taylor, J. M. Hendrickx, and Francois Glineur. "Exact worst-case performance of first-order methods for composite convex optimization." In: *SIAM J. Optim.* 27.3 (Jan. 2017), 1283–313. DOI: [10.1137/16m108104x](https://doi.org/10.1137/16m108104x) (cit. on pp. 21, 24, 25).
- [76] D. Kim and J. A. Fessler. "Adaptive restart of the optimized gradient method for convex optimization." In: *J. Optim. Theory Appl.* 178.1 (July 2018), 240–63. DOI: [10.1007/s10957-018-1287-4](https://doi.org/10.1007/s10957-018-1287-4) (cit. on pp. 21, 24, 25).
- [77] I. Daubechies, M. Defrise, and C. De Mol. "An iterative thresholding algorithm for linear inverse problems with a sparsity constraint." In: *Comm. Pure Appl. Math.* 57.11 (Nov. 2004), 1413–57. DOI: [10.1002/cpa.20042](https://doi.org/10.1002/cpa.20042) (cit. on p. 23).
- [78] P. Combettes and V. Wajs. "Signal recovery by proximal forward-backward splitting." In: *SIAM J. Multi. Mod. Sim.* 4.4 (2005), 1168–200. DOI: [10.1137/050626090](https://doi.org/10.1137/050626090) (cit. on p. 23).
- [79] M. J. Muckley, D. C. Noll, and J. A. Fessler. "Fast parallel MR image reconstruction via B1-based, adaptive restart, iterative soft thresholding algorithms (BARISTA)." In: *IEEE Trans. Med. Imag.* 34.2 (Feb. 2015), 578–88. DOI: [10.1109/TMI.2014.2363034](https://doi.org/10.1109/TMI.2014.2363034) (cit. on p. 23).
- [80] A. Beck and M. Teboulle. "A fast iterative shrinkage-thresholding algorithm for linear inverse problems." In: *SIAM J. Imaging Sci.* 2.1 (2009), 183–202. DOI: [10.1137/080716542](https://doi.org/10.1137/080716542) (cit. on p. 23).
- [81] A. Beck and M. Teboulle. "Fast gradient-based algorithms for constrained total variation image denoising and deblurring problems." In: *IEEE Trans. Im. Proc.* 18.11 (Nov. 2009), 2419–34. DOI: [10.1109/TIP.2009.2028250](https://doi.org/10.1109/TIP.2009.2028250) (cit. on pp. 23, 28).
- [82] L. El Gueddari et al. "Self-calibrating nonlinear reconstruction algorithms for variable density sampling and parallel reception MRI." In: *Proc. IEEE SAM.* 2018, 415–9. DOI: [10.1109/SAM.2018.8448776](https://doi.org/10.1109/SAM.2018.8448776) (cit. on p. 24).

- [83] C. Y. Lin and J. A. Fessler. "Accelerated methods for low-rank plus sparse image reconstruction." In: *Proc. IEEE Intl. Symp. Biomed. Imag.* 2018, 48–51. DOI: [10.1109/ISBI.2018.8363520](https://doi.org/10.1109/ISBI.2018.8363520) (cit. on p. 24).
- [84] C. Y. Lin and J. A. Fessler. "Efficient dynamic parallel MRI reconstruction for the low-rank plus sparse model." In: *IEEE Trans. Computational Imaging* 5.1 (Mar. 2019), 17–26. DOI: [10.1109/TCI.2018.2882089](https://doi.org/10.1109/TCI.2018.2882089) (cit. on p. 24).
- [85] Z. Ramzi, P. Ciuciu, and J-L. Starck. "Benchmarking proximal methods acceleration enhancements for CS-acquired MR image analysis reconstruction." In: *Sig. Proc. with Adapt. Sparse Struct. Rep. SPARS.* 2019. URL: <https://hal.inria.fr/hal-02298569> (cit. on p. 24).
- [86] B. O'Donoghue and E. Candes. "Adaptive restart for accelerated gradient schemes." In: *Found. Comp. Math.* 15.3 (June 2015), 715–32. DOI: [10.1007/s10208-013-9150-3](https://doi.org/10.1007/s10208-013-9150-3) (cit. on p. 24).
- [87] J. Liang and C-B. Schonlieb. *Faster FISTA*. 2018. URL: <http://arxiv.org/abs/1807.04005> (cit. on p. 24).
- [88] J. Liang and C-B. Schonlieb. *Improving FISTA: Faster, smarter and greedier*. 2018. URL: <http://arxiv.org/abs/1811.01430> (cit. on p. 24).
- [89] A. Chambolle. "An algorithm for total variation minimization and applications." In: *J. Math. Im. Vision* 20.1-2 (Jan. 2004), 89–97. DOI: [10.1023/B:JMIV.0000011325.36760.1e](https://doi.org/10.1023/B:JMIV.0000011325.36760.1e) (cit. on p. 28).
- [90] Y. Wang et al. "A new alternating minimization algorithm for total variation image reconstruction." In: *SIAM J. Imaging Sci.* 1.3 (2008), 248–72. DOI: [10.1137/080724265](https://doi.org/10.1137/080724265) (cit. on p. 29).
- [91] T. Goldstein and S. Osher. "The split Bregman method for L1-regularized problems." In: *SIAM J. Imaging Sci.* 2.2 (2009), 323–43. DOI: [10.1137/080725891](https://doi.org/10.1137/080725891) (cit. on p. 30).
- [92] J. Aelterman et al. "Augmented Lagrangian based reconstruction of non-uniformly sub-Nyquist sampled MRI data." In: *Signal Processing* 91.12 (Jan. 2011), 2731–42. DOI: [10.1016/j.sigpro.2011.04.033](https://doi.org/10.1016/j.sigpro.2011.04.033) (cit. on p. 30).

- [93] J. Eckstein and D. P. Bertsekas. "On the Douglas-Rachford splitting method and the proximal point algorithm for maximal monotone operators." In: *Mathematical Programming* 55.1-3 (Apr. 1992), 293–318. DOI: [10.1007/BF01581204](https://doi.org/10.1007/BF01581204) (cit. on p. 30).
- [94] S. Boyd et al. "Distributed optimization and statistical learning via the alternating direction method of multipliers." In: *Found. & Trends in Machine Learning* 3.1 (2010), 1–122. DOI: [10.1561/2200000016](https://doi.org/10.1561/2200000016) (cit. on pp. 30, 32).
- [95] Z. Xu, M. A. T. Figueiredo, and T. Goldstein. "Adaptive ADMM with spectral penalty parameter selection." In: *aistats.* 2017, 718–27. URL: <http://proceedings.mlr.press/v54/xu17a.html> (cit. on p. 32).
- [96] B. Wohlberg. *ADMM penalty parameter selection by residual balancing*. 2017. URL: <http://arxiv.org/abs/1704.06209> (cit. on p. 32).
- [97] J. Eckstein. "Parallel alternating direction multiplier decomposition of convex programs." In: *J. Optim. Theory Appl.* 80.1 (Jan. 1994), 39–62. DOI: [10.1007/BF02196592](https://doi.org/10.1007/BF02196592) (cit. on p. 32).
- [98] M. Le and J. A. Fessler. "Efficient, convergent SENSE MRI reconstruction for non-periodic boundary conditions via tridiagonal solvers." In: *IEEE Trans. Computational Imaging* 3.1 (Mar. 2017), 11–21. DOI: [10.1109/TCI.2016.2626999](https://doi.org/10.1109/TCI.2016.2626999) (cit. on pp. 32, 33).
- [99] Y. Chen et al. "Fast algorithms for image reconstruction with application to partially parallel MR imaging." In: *SIAM J. Imaging Sci.* 5.1 (2012), 90–118. DOI: [10.1137/100792688](https://doi.org/10.1137/100792688) (cit. on pp. 33, 34).
- [100] A. Chambolle and T. Pock. "A first-order primal-dual algorithm for convex problems with applications to imaging." In: *J. Math. Im. Vision* 40.1 (2011), 120–145. DOI: [10.1007/s10851-010-0251-1](https://doi.org/10.1007/s10851-010-0251-1) (cit. on p. 34).
- [101] T. Pock and A. Chambolle. "Diagonal preconditioning for first order primal-dual algorithms in convex optimization." In: *Proc. Intl. Conf. Comp. Vision.* 2011, 1762–9. DOI: [10.1109/ICCV.2011.6126441](https://doi.org/10.1109/ICCV.2011.6126441) (cit. on p. 34).
- [102] P. L. Combettes and J. C. Pesquet. "Primal-dual splitting algorithm for solving inclusions with mixtures of composite, Lipschitzian, and parallel-sum type monotone operators." In: *Set-Valued Var Anal* 20.2 (June 2012), 307–30. DOI: [10.1007/s11228-011-0191-y](https://doi.org/10.1007/s11228-011-0191-y) (cit. on p. 34).

- [103] L. Condat. "A primal-dual splitting method for convex optimization involving Lipschitzian, proximable and linear composite terms." In: *J. Optim. Theory Appl.* 158.2 (2013), 460–79. DOI: [10.1007/s10957-012-0245-9](https://doi.org/10.1007/s10957-012-0245-9) (cit. on p. 34).
- [104] E. Y. Sidky, J. H. Jorgensen, and X. Pan. "Convex optimization problem prototyping for image reconstruction in computed tomography with the Chambolle-Pock algorithm." In: *Phys. Med. Biol.* 57.10 (May 2012), 3065–92. DOI: [10.1088/0031-9155/57/10/3065](https://doi.org/10.1088/0031-9155/57/10/3065) (cit. on p. 34).
- [105] B. CÔNG VU. "A splitting algorithm for dual monotone inclusions involving cocoercive operators." In: *Adv. in Comp. Math.* 38.3 (Apr. 2013), 667–81. DOI: [10.1007/s10444-011-9254-8](https://doi.org/10.1007/s10444-011-9254-8) (cit. on p. 34).
- [106] T. Valkonen. "A primal-dual hybrid gradient method for nonlinear operators with applications to MRI." In: *Inverse Prob.* 30.5 (May 2014), p. 055012. DOI: [10.1088/0266-5611/30/5/055012](https://doi.org/10.1088/0266-5611/30/5/055012) (cit. on p. 34).
- [107] F. Ong, M. Uecker, and M. Lustig. *Accelerating non-Cartesian MRI reconstruction convergence using k-space preconditioning*. 2019. URL: <http://arxiv.org/abs/1902.09657> (cit. on p. 34).
- [108] M. Lustig and J. M. Pauly. "SPIRiT: Iterative self-consistent parallel imaging reconstruction from arbitrary k-space." In: *Mag. Res. Med.* 64.2 (Aug. 2010), 457–71. DOI: [10.1002/mrm.22428](https://doi.org/10.1002/mrm.22428) (cit. on pp. 37, 71).
- [109] M. Murphy et al. "Fast ℓ_1 -SPIRiT compressed sensing parallel imaging MRI: scalable parallel implementation and clinically feasible runtime." In: *IEEE Trans. Med. Imag.* 31.6 (June 2012), 1250–62. DOI: [10.1109/TMI.2012.2188039](https://doi.org/10.1109/TMI.2012.2188039) (cit. on p. 37).
- [110] D. Weller, S. Ramani, and J. A. Fessler. "Augmented Lagrangian with variable splitting for faster non-Cartesian L1-SPIRiT MR image reconstruction." In: *IEEE Trans. Med. Imag.* 33.2 (Feb. 2014), 351–61. DOI: [10.1109/TMI.2013.2285046](https://doi.org/10.1109/TMI.2013.2285046) (cit. on p. 37).
- [111] J. Duan, Y. Liu, and P. Jing. "Efficient operator splitting algorithm for joint sparsity-regularized SPIRiT-based parallel MR imaging reconstruction." In: *Mag. Res. Im.* 46 (Feb. 2018), 81–9. DOI: [10.1016/j.mri.2017.10.013](https://doi.org/10.1016/j.mri.2017.10.013) (cit. on p. 37).
- [112] M. Uecker et al. "ESPIRiT—an eigenvalue approach to autocalibrating parallel MRI: Where SENSE meets GRAPPA." In: *Mag. Res. Med.* 71.3 (Mar. 2014), 990–1001. DOI: [10.1002/mrm.24751](https://doi.org/10.1002/mrm.24751) (cit. on p. 38).

- [113] L. El Gueddari et al. "Calibrationless OSCAR-based image reconstruction in compressed sensing parallel MRI." In: *Proc. IEEE Intl. Symp. Biomed. Imag.* 2019, 1532–6 (cit. on p. 38).
- [114] S. Ravishankar and Y. Bresler. "MR image reconstruction from highly undersampled k-space data by dictionary learning." In: *IEEE Trans. Med. Imag.* 30.5 (May 2011), 1028–41. DOI: [10.1109/TMI.2010.2090538](https://doi.org/10.1109/TMI.2010.2090538) (cit. on pp. 42, 51, 71, 72).
- [115] S. Ravishankar and Y. Bresler. "Efficient blind compressed sensing using sparsifying transforms with convergence guarantees and application to MRI." In: *SIAM J. Imaging Sci.* 8.4 (2015), 2519–57. DOI: [10.1137/141002293](https://doi.org/10.1137/141002293) (cit. on pp. 43, 51).
- [116] I. Y. Chun and J. A. Fessler. "Convolutional dictionary learning: acceleration and convergence." In: *IEEE Trans. Im. Proc.* 27.4 (Apr. 2018), 1697–712. DOI: [10.1109/TIP.2017.2761545](https://doi.org/10.1109/TIP.2017.2761545) (cit. on pp. 46, 48).
- [117] I. Y. Chun and J. A. Fessler. *Convolutional analysis operator learning: acceleration and convergence*. 2018. URL: <http://arxiv.org/abs/1802.05584> (cit. on pp. 46, 47).
- [118] T. Nguyen-Duc and W-K. Jeong. "Compressed sensing dynamic MRI reconstruction using multi-scale 3D convolutional sparse coding with elastic net regularization." In: *Proc. IEEE Intl. Symp. Biomed. Imag.* 2018, 332–5. DOI: [10.1109/ISBI.2018.8363586](https://doi.org/10.1109/ISBI.2018.8363586) (cit. on p. 46).
- [119] B. Wohlberg. "Efficient algorithms for convolutional sparse representations." In: *IEEE Trans. Im. Proc.* 25.1 (Jan. 2016), 301–15. DOI: [10.1109/TIP.2015.2495260](https://doi.org/10.1109/TIP.2015.2495260) (cit. on p. 46).
- [120] A. Lahiri, S. Ravishankar, and J. A. Fessler. "Combining supervised and semi-blind dictionary (Super-BReD) learning for MRI reconstruction." In: *Proc. Intl. Soc. Mag. Res. Med.* To appear. 2020, p. 3456 (cit. on p. 51).
- [121] G. Wang et al. "Image reconstruction is a new frontier of machine learning." In: *IEEE Trans. Med. Imag.* 37.6 (June 2018), 1289–96. DOI: [10.1109/TMI.2018.2833635](https://doi.org/10.1109/TMI.2018.2833635) (cit. on p. 52).
- [122] M. Aharon, M. Elad, and A. Bruckstein. "K-SVD: an algorithm for designing overcomplete dictionaries for sparse representation." In: *IEEE Trans. Sig. Proc.* 54.11 (Nov. 2006), 4311–22. DOI: [10.1109/TSP.2006.881199](https://doi.org/10.1109/TSP.2006.881199) (cit. on p. 58).

- [123] S. Ravishankar and Y. Bresler. " ℓ_0 sparsifying transform learning with efficient optimal updates and convergence guarantees." In: *IEEE Trans. Sig. Proc.* 63.9 (May 2015), 2389–404. DOI: [10.1109/TSP.2015.2405503](https://doi.org/10.1109/TSP.2015.2405503) (cit. on p. 58).
- [124] X. Zheng et al. "PWLS-ULTRA: An efficient clustering and learning-based approach for low-dose 3D CT image reconstruction." In: *IEEE Trans. Med. Imag.* 37.6 (June 2018), 1498–510. DOI: [10.1109/TMI.2018.2832007](https://doi.org/10.1109/TMI.2018.2832007) (cit. on pp. 60, 61, 64, 65).
- [125] H. Nien and J. A. Fessler. "Relaxed linearized algorithms for faster X-ray CT image reconstruction." In: *IEEE Trans. Med. Imag.* 35.4 (Apr. 2016), 1090–8. DOI: [10.1109/TMI.2015.2508780](https://doi.org/10.1109/TMI.2015.2508780) (cit. on p. 60).
- [126] S. Ravishankar and Y. Bresler. "Data-driven learning of a union of sparsifying transforms model for blind compressed sensing." In: *IEEE Trans. Computational Imaging* 2.3 (Sept. 2016), 294–309. DOI: [10.1109/TCI.2016.2567299](https://doi.org/10.1109/TCI.2016.2567299) (cit. on pp. 63, 94).
- [127] S. Ravishankar, R. R. Nadakuditi, and J. A. Fessler. "Efficient sum of outer products dictionary learning (SOUP-DIL) and its application to inverse problems." In: *IEEE Trans. Computational Imaging* 3.4 (Dec. 2017), 694–709. DOI: [10.1109/TCI.2017.2697206](https://doi.org/10.1109/TCI.2017.2697206) (cit. on pp. 68, 69, 71, 72).
- [128] X. Qu et al. "Magnetic resonance image reconstruction from undersampled measurements using a patch-based nonlocal operator." In: *Med. Im. Anal.* 18.6 (Aug. 2014), 843–56. DOI: [10.1016/j.media.2013.09.007](https://doi.org/10.1016/j.media.2013.09.007) (cit. on pp. 71, 72).
- [129] Z. Zhan et al. "Fast multiclass dictionaries learning with geometrical directions in MRI reconstruction." In: *IEEE Trans. Biomed. Engin.* 63.9 (Sept. 2016), 1850–61. DOI: [10.1109/tbme.2015.2503756](https://doi.org/10.1109/tbme.2015.2503756) (cit. on p. 72).
- [130] A. Buades, B. Coll, and J-M. Morel. "The staircasing effect in neighborhood filters and its solution." In: *IEEE Trans. Im. Proc.* 15.6 (June 2006), 1499–505. DOI: [10.1109/TIP.2006.871137](https://doi.org/10.1109/TIP.2006.871137) (cit. on p. 74).
- [131] K. Dabov et al. "Image denoising by sparse 3-D transform-domain collaborative filtering." In: *IEEE Trans. Im. Proc.* 16.8 (Aug. 2007), 2080–95. DOI: [10.1109/TIP.2007.901238](https://doi.org/10.1109/TIP.2007.901238) (cit. on p. 74).
- [132] S. H. Chan, X. Wang, and O. A. Elgendy. "Plug-and-play ADMM for image restoration: fixed-point convergence and applications." In: *IEEE Trans. Computational Imaging* 3.1 (Mar. 2017), 84–98. DOI: [10.1109/tci.2016.2629286](https://doi.org/10.1109/tci.2016.2629286) (cit. on p. 74).

- [133] G. T. Buzzard et al. "Plug-and-play unplugged: optimization-free reconstruction using consensus equilibrium." In: *SIAM J. Imaging Sci.* 11.3 (Jan. 2018), 2001–20. DOI: [10.1137/17m1122451](https://doi.org/10.1137/17m1122451) (cit. on p. 74).
- [134] Y. Romano, M. Elad, and P. Milanfar. "The little engine that could: Regularization by denoising (RED)." In: *SIAM J. Imaging Sci.* 10.4 (2017), 1804–44. DOI: [10.1137/16M1102884](https://doi.org/10.1137/16M1102884) (cit. on p. 74).
- [135] E. T. Reehorst and P. Schniter. *Regularization by denoising: clarifications and new interpretations*. 2018. URL: <http://arxiv.org/abs/1806.02296> (cit. on p. 74).
- [136] R. Ahmad et al. "Plug and play methods for magnetic resonance imaging." In: *IEEE Sig. Proc. Mag.* 37.1 (Jan. 2020), 105–16. DOI: [10.1109/MSP.2019.2949470](https://doi.org/10.1109/MSP.2019.2949470) (cit. on p. 74).
- [137] S. Wang et al. "Exploiting deep convolutional neural network for fast magnetic resonance imaging." In: *Proc. Intl. Soc. Mag. Res. Med.* 2016, p. 1778. URL: <http://archive.ismrm.org/2016/1778.html> (cit. on pp. 77, 81).
- [138] D. Lee, J. Yoo, and J. C. Ye. *Deep artifact learning for compressed sensing and parallel MRI*. 2017. URL: <http://arxiv.org/abs/1703.01120> (cit. on p. 77).
- [139] M. Akcakaya et al. "Scan-specific robust artificial-neural-networks for k-space interpolation (RAKI) reconstruction: Database-free deep learning for fast imaging." In: *Mag. Res. Med.* 81.1 (Jan. 2019), 439–53. DOI: [10.1002/mrm.27420](https://doi.org/10.1002/mrm.27420) (cit. on p. 77).
- [140] Y. Han and J. C. Ye. "K-space deep learning for accelerated MRI." In: *IEEE Trans. Med. Imag.* 39.2 (Feb. 2020), 377–86. DOI: [10.1109/TMI.2019.2927101](https://doi.org/10.1109/TMI.2019.2927101) (cit. on p. 77).
- [141] B. Zhu et al. "Image reconstruction by domain-transform manifold learning." In: *Nature* 555 (Mar. 2018), 487–92. DOI: [10.1038/nature25988](https://doi.org/10.1038/nature25988) (cit. on p. 77).
- [142] Y. Yang et al. "Deep ADMM-net for compressive sensing MRI." In: *Neural Info. Proc. Sys.* 2016, 10–18. URL: <https://papers.nips.cc/paper/6406-deep-admm-net-for-compressive-sensing-mri> (cit. on pp. 77, 85).

- [143] K. Hammernik et al. "Learning a variational network for reconstruction of accelerated MRI data." In: *Mag. Res. Med.* 79.6 (June 2018), 3055–71. DOI: [10.1002/mrm.26977](https://doi.org/10.1002/mrm.26977) (cit. on pp. 77, 85).
- [144] J. Schlemper et al. "A deep cascade of convolutional neural networks for dynamic MR image reconstruction." In: *IEEE Trans. Med. Imag.* 37.2 (Feb. 2018), 491–503. DOI: [10.1109/tmi.2017.2760978](https://doi.org/10.1109/tmi.2017.2760978) (cit. on pp. 77, 102).
- [145] T. M. Quan, T. Nguyen-Duc, and W-K. Jeong. "Compressed sensing MRI reconstruction using a generative adversarial network with a cyclic loss." In: *IEEE Trans. Med. Imag.* 37.6 (June 2018), 1488–97. DOI: [10.1109/TMI.2018.2820120](https://doi.org/10.1109/TMI.2018.2820120) (cit. on p. 77).
- [146] D. Lee et al. "Deep residual learning for accelerated MRI using magnitude and phase networks." In: *IEEE Trans. Biomed. Engin.* 65.9 (Sept. 2018), 1985–95. DOI: [10.1109/TBME.2018.2821699](https://doi.org/10.1109/TBME.2018.2821699) (cit. on p. 77).
- [147] G. Nataraj and R. Otazo. "Investigating robustness to unseen pathologies in model-free deep multicoil reconstruction." In: *ISMRM Workshop on Data Sampling and Image Reconstruction*. 2020 (cit. on p. 79).
- [148] G. Yang et al. "DAGAN: Deep de-aliasing generative adversarial networks for fast compressed sensing MRI reconstruction." In: *IEEE Trans. Med. Imag.* 37.6 (June 2018), 1310–21. DOI: [10.1109/TMI.2017.2785879](https://doi.org/10.1109/TMI.2017.2785879) (cit. on p. 81).
- [149] K. He et al. "Deep residual learning for image recognition." In: *Proc. IEEE Conf. on Comp. Vision and Pattern Recognition*. 2016, 770–8. DOI: [10.1109/CVPR.2016.90](https://doi.org/10.1109/CVPR.2016.90) (cit. on pp. 81, 91).
- [150] K. Zhang et al. "Beyond a Gaussian denoiser: residual learning of deep CNN for image denoising." In: *IEEE Trans. Im. Proc.* 26.7 (July 2017), 3142–55. DOI: [10.1109/tip.2017.2662206](https://doi.org/10.1109/tip.2017.2662206) (cit. on p. 81).
- [151] K. Gregor and Y. LeCun. "Learning fast approximations of sparse coding." In: *Proc. Intl. Conf. Mach. Learn.* 2010. URL: <http://yann.lecun.com/exdb/publis/pdf/gregor-icml-10.pdf> (cit. on p. 85).
- [152] T. Meinhardt et al. "Learning proximal operators: using denoising networks for regularizing inverse imaging problems." In: *Proc. Intl. Conf. Comp. Vision*. 2017, 1799–808. DOI: [10.1109/ICCV.2017.198](https://doi.org/10.1109/ICCV.2017.198) (cit. on p. 85).

- [153] U. Schmidt and S. Roth. "Shrinkage fields for effective image restoration." In: *Proc. IEEE Conf. on Comp. Vision and Pattern Recognition*. 2014, 2774–81. DOI: [10.1109/CVPR.2014.349](https://doi.org/10.1109/CVPR.2014.349) (cit. on p. 85).
- [154] Y. Chen, W. Yu, and T. Pock. "On learning optimized reaction diffusion processes for effective image restoration." In: *Proc. IEEE Conf. on Comp. Vision and Pattern Recognition*. 2015, 5261–9. DOI: [10.1109/CVPR.2015.7299163](https://doi.org/10.1109/CVPR.2015.7299163) (cit. on p. 85).
- [155] Y. Chen and T. Pock. "Trainable nonlinear reaction diffusion: A flexible framework for fast and effective image restoration." In: *IEEE Trans. Patt. Anal. Mach. Int.* 39.6 (June 2017), 1256–72. DOI: [10.1109/TPAMI.2016.2596743](https://doi.org/10.1109/TPAMI.2016.2596743) (cit. on p. 85).
- [156] K. Hammerl et al. "Learning a variational model for compressed sensing MRI reconstruction." In: *Proc. Intl. Soc. Mag. Res. Med.* 2016, p. 1088. URL: <http://archive.ismrm.org/2016/1088.html> (cit. on p. 85).
- [157] Y. Yang et al. *ADMM-net: A deep learning approach for compressive sensing MRI*. 2017. URL: <http://arxiv.org/abs/1705.06869> (cit. on p. 85).
- [158] B. Xin et al. *Maximal sparsity with deep networks?* 2016. URL: <http://arxiv.org/abs/1605.01636> (cit. on p. 85).
- [159] P. Schniter. "Recent advances in approximate message passing." In: *spars-17*. 2017, plenary (cit. on p. 85).
- [160] H-Y. Liu et al. "Compressive imaging with iterative forward models." In: *Proc. IEEE Conf. Acoust. Speech Sig. Proc.* 2017 (cit. on p. 85).
- [161] J. Adler and O. Oktem. "Learned primal-dual reconstruction." In: *IEEE Trans. Med. Imag.* 37.6 (June 2018), 1322–32. DOI: [10.1109/tmi.2018.2799231](https://doi.org/10.1109/tmi.2018.2799231) (cit. on p. 85).
- [162] Y. Malitsky and T. Pock. "A first-order primal-dual algorithm with linesearch." In: *SIAM J. Optim.* 28.1 (Jan. 2018), 411–32. DOI: [10.1137/16m1092015](https://doi.org/10.1137/16m1092015) (cit. on p. 85).
- [163] S. Ravishankar et al. "Deep dictionary-transform learning for image reconstruction." In: *Proc. IEEE Intl. Symp. Biomed. Imag.* 2018, 1208–12. DOI: [10.1109/ISBI.2018.8363788](https://doi.org/10.1109/ISBI.2018.8363788) (cit. on pp. 85, 93).
- [164] I. Y. Chun and J. A. Fessler. "Deep BCD-net using identical encoding-decoding CNN structures for iterative image recovery." In: *Proc. IEEE Wkshp. on Image, Video, Multidim. Signal Proc.* 2018, 1–5. DOI: [10.1109/IVMSPW.2018.8448694](https://doi.org/10.1109/IVMSPW.2018.8448694) (cit. on p. 85).

- [165] I. Y. Chun and J. A. Fessler. *Deep BCD-net using identical encoding-decoding CNN structures for iterative image recovery*. 2018. URL: <http://arxiv.org/abs/1802.07129> (cit. on p. 85).
- [166] H. Lim et al. "Application of trained deep BCD-net to iterative low-count PET image reconstruction." In: *Proc. IEEE Nuc. Sci. Symp. Med. Im. Conf.* 2018, 1–4. DOI: [10.1109/NSSMIC.2018.8824563](https://doi.org/10.1109/NSSMIC.2018.8824563) (cit. on p. 85).
- [167] I. Y. Chun et al. "Fast and convergent iterative image recovery using trained convolutional neural networks." In: *Allerton Conf. on Comm., Control, and Computing. Invited.* 2018, 155–9. DOI: [10.1109/ALLERTON.2018.8635932](https://doi.org/10.1109/ALLERTON.2018.8635932) (cit. on p. 85).
- [168] J. R. Hershey, J. L. Roux, and F. Weninger. *Deep unfolding: Model-based inspiration of novel deep architectures*. 2014. URL: <http://arxiv.org/abs/1409.2574> (cit. on p. 85).
- [169] H. K. Aggarwal, M. P. Mani, and M. Jacob. "Model based image reconstruction using deep learned priors (MODL)." In: *Proc. IEEE Intl. Symp. Biomed. Imag.* 2018, 671–4. DOI: [10.1109/ISBI.2018.8363663](https://doi.org/10.1109/ISBI.2018.8363663) (cit. on pp. 85, 91).
- [170] K. H. Jin, M. McCann, and M. Unser. "BPConvNet for compressed sensing recovery in bioimaging." In: *spars-17*. 2017 (cit. on p. 85).
- [171] H. Chen et al. "LEARN: Learned experts: assessment-based reconstruction network for sparse-data CT." In: *IEEE Trans. Med. Imag.* 37.6 (June 2018), 1333–47. DOI: [10.1109/TMI.2018.2805692](https://doi.org/10.1109/TMI.2018.2805692) (cit. on p. 85).
- [172] D. Wu et al. *End-to-end abnormality detection in medical imaging*. 2018. URL: <http://arxiv.org/abs/1711.02074> (cit. on p. 85).
- [173] D. Liang et al. "Deep MRI reconstruction: Unrolled optimization algorithms meet neural networks." In: *IEEE Sig. Proc. Mag.* 37.1 (Jan. 2020), 141–51. DOI: [10.1109/MSP.2019.2950557](https://doi.org/10.1109/MSP.2019.2950557) (cit. on p. 85).
- [174] V. Monga, Y. Li, and Y. C. Eldar. *Algorithm unrolling: interpretable, efficient deep learning for signal and image processing*. 2020. URL: <http://arxiv.org/abs/1912.10557> (cit. on p. 85).
- [175] I. J. Goodfellow et al. *Generative adversarial networks*. 2014. URL: <http://arxiv.org/abs/1406.2661> (cit. on pp. 86, 87).

- [176] X. Chen et al. "InfoGAN: interpretable representation learning by information maximizing generative adversarial nets." In: *Neural Info. Proc. Sys.* 2016, 2172–80. URL: <https://papers.nips.cc/paper/6399-infogan-interpretable-representation-learning-by-information-maximizing-generative-adversarial-nets> (cit. on pp. 86, 87).
- [177] A. Bora et al. "Compressed sensing using generative models." In: *Proc. Intl. Conf. Mach. Learn.* Vol. 70. 2017, 537–46. URL: <http://proceedings.mlr.press/v70/bora17a.html> (cit. on pp. 86, 87).
- [178] S. Kolouri et al. *Sliced-Wasserstein autoencoder: an embarrassingly simple generative model*. 2018. URL: <http://arxiv.org/abs/1804.01947> (cit. on p. 88).
- [179] D. Berthelot, T. Schumm, and L. Metz. *BEGAN: boundary equilibrium generative adversarial networks*. 2017. URL: <http://arxiv.org/abs/1703.10717> (cit. on pp. 89, 90).
- [180] B. Yaman et al. "Self-supervised learning of physics-based reconstruction neural networks without fully-sampled reference data." In: *Mag. Res. Med.* (2020). DOI: [10.1002/mrm.28378](https://doi.org/10.1002/mrm.28378) (cit. on p. 92).
- [181] V. Antun et al. *On instabilities of deep learning in image reconstruction - Does AI come at a cost?* 2019. URL: <http://arxiv.org/abs/1902.05300> (cit. on p. 92).
- [182] E. Haneda et al. "CT sinogram analysis using deep learning." In: *Proc. 5th Intl. Mtg. on Image Formation in X-ray CT*. 2018, 419–22 (cit. on p. 105).
- [183] Q. De Man et al. "A two-dimensional feasibility study of deep learning-based feature detection and characterization directly from CT sinograms." In: *Med. Phys.* 46.12 (Dec. 2019), e790–800. DOI: [10.1002/mp.13640](https://doi.org/10.1002/mp.13640) (cit. on p. 105).
- [184] B. Gozcu et al. "Learning-based compressive MRI." In: *IEEE Trans. Med. Imag.* 37.6 (June 2018), 1394–406. DOI: [10.1109/TMI.2018.2832540](https://doi.org/10.1109/TMI.2018.2832540) (cit. on p. 107).